

What do you do with a quantum state once you've prepared one?

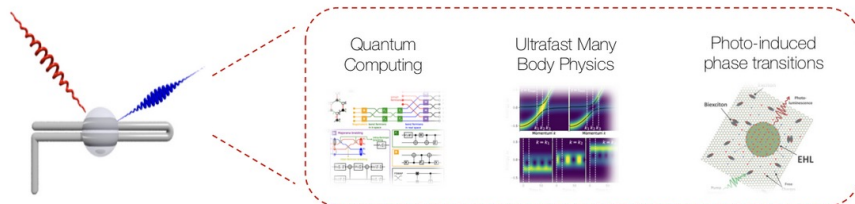
Alexander (Lex) Kemper



Department of Physics
North Carolina State University
<https://go.ncsu.edu/kemper-lab>

LANL QC Summer School
06/27/2023





Kemper Lab

Quantum materials in and out of equilibrium.

Collaborations with:

- Jim Freericks (Georgetown)
- Bert de Jong, Katie Klymko, Daan Camps, Roel van Beeument, Akhil Francis (LBNL)
- Thomas Steckmann (UMD)

Current members



Alexander (Lex)
Kemper
Principal investigator



Efekan Kökcü
Graduate Researcher



Anjali Agrawal
Graduate Researcher



Heba Labib
Graduate Researcher



Jack Howard
Undergraduate
Researcher



Natalia Wilson
Undergraduate
Researcher



Daniel Brandon
Undergraduate
Researcher



Sarah Klas
Undergraduate
Researcher



Norman Hogan
Graduate Researcher



Ethan Blair
Undergraduate
Researcher

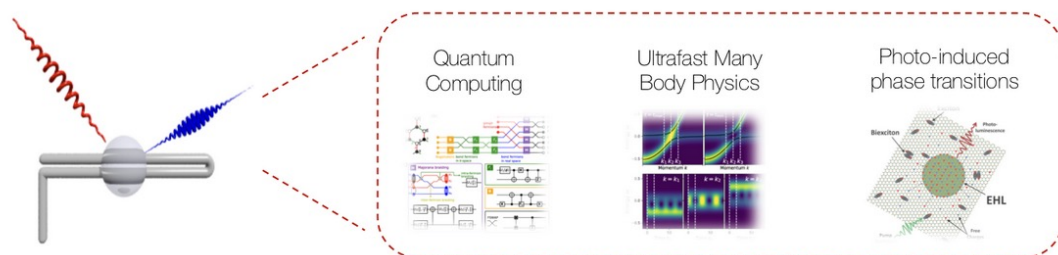


Your Name
New lab member

Brief outline

- Quantum Matter meets Quantum Computing
- Response functions
 - Why we care
 - How do find them
- A new paradigm: Making the experiment part of the simulation via linear response

Why quantum computing for condensed matter?

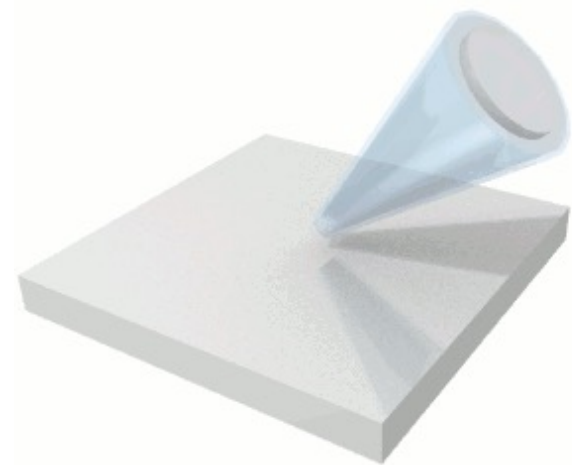


Kemper Lab

Quantum materials in and out of equilibrium.

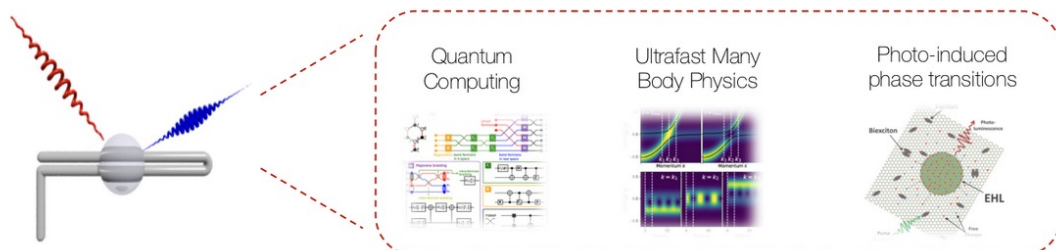


Time-resolved experiments



Shen group (Stanford)

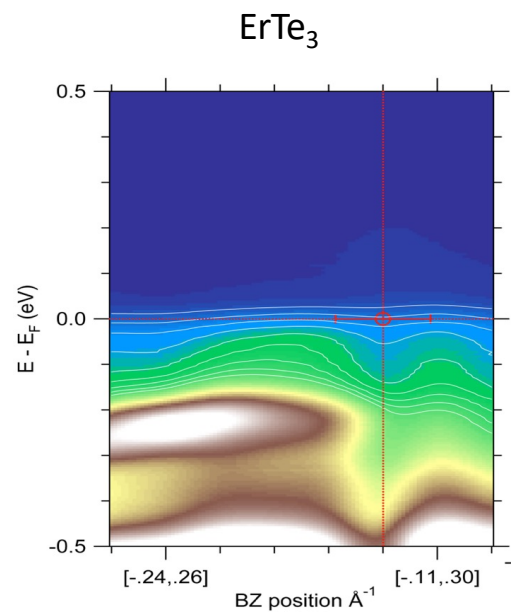
Why quantum computing for condensed matter?



Kemper Lab

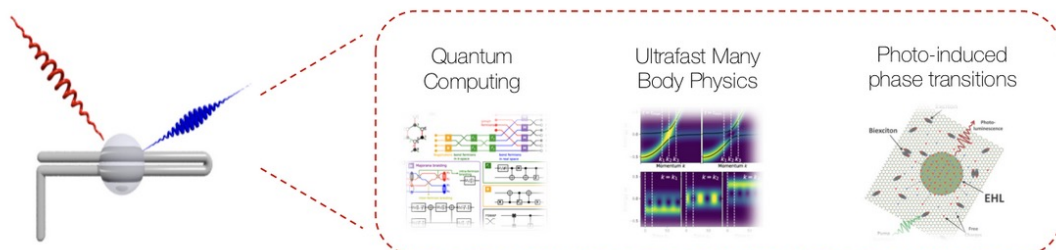
Quantum materials in and out of equilibrium.

Time-resolved experiments



Shen group (Stanford)

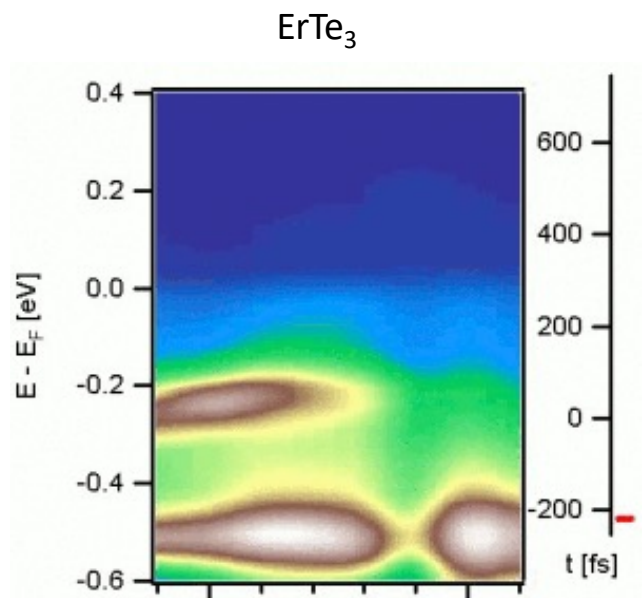
Why quantum computing for condensed matter?



Kemper Lab

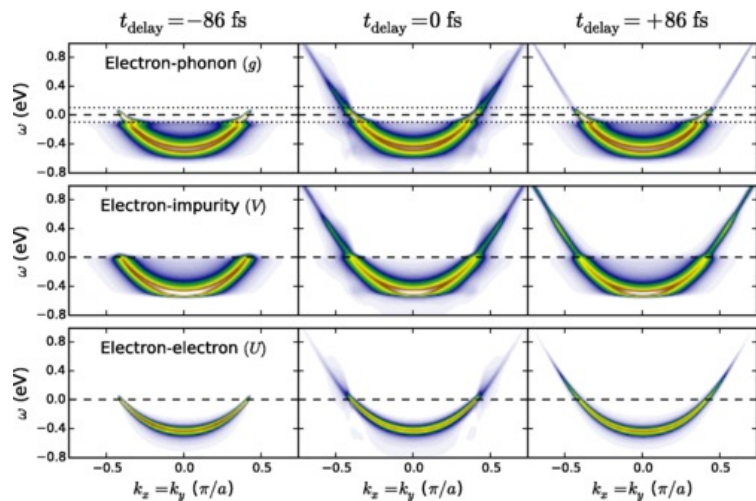
Quantum materials in and out of equilibrium.

Time-resolved experiments



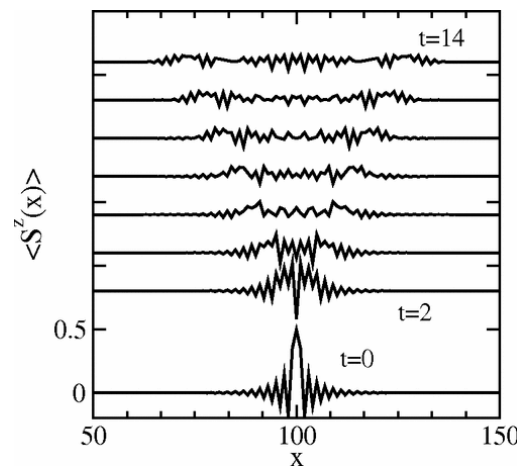
Shen group (Stanford)

Why quantum computing for condensed matter?



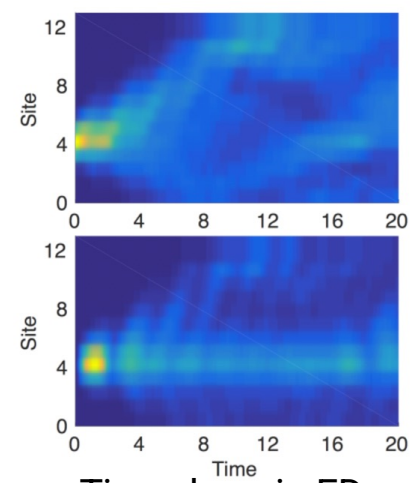
Non-Equilibrium Green's functions

Phys. Rev. X 8, 041009 (2018)



Time domain DMRG

Phys. Rev. Lett. 93, 076401 (2004)



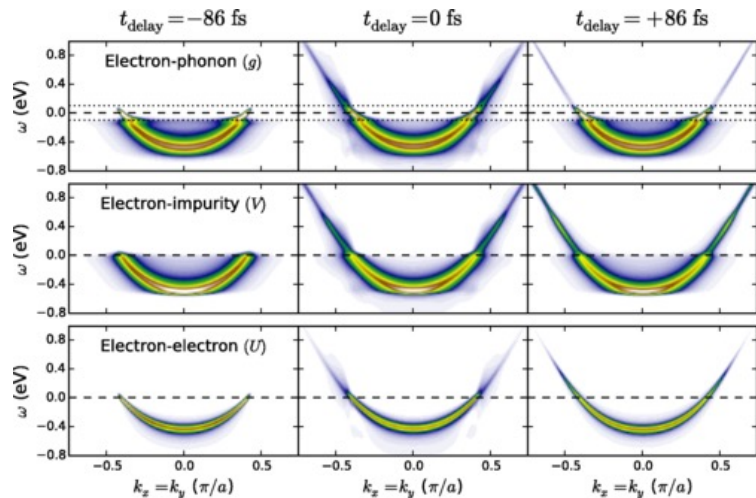
Time domain ED

Johnston & Kemper, unpublished

Why quantum computing for condensed matter?

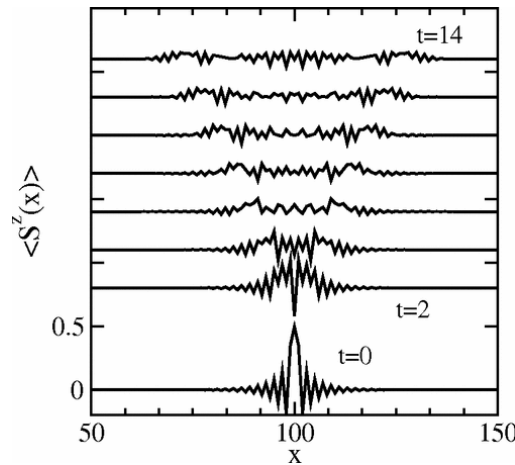


All these techniques eventually reach a barrier.

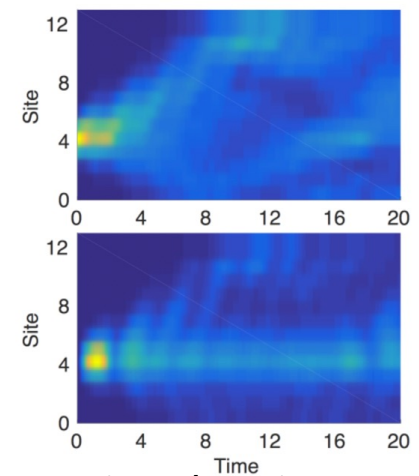


Non-Equilibrium Green's functions

Phys. Rev. X 8, 041009 (2018)



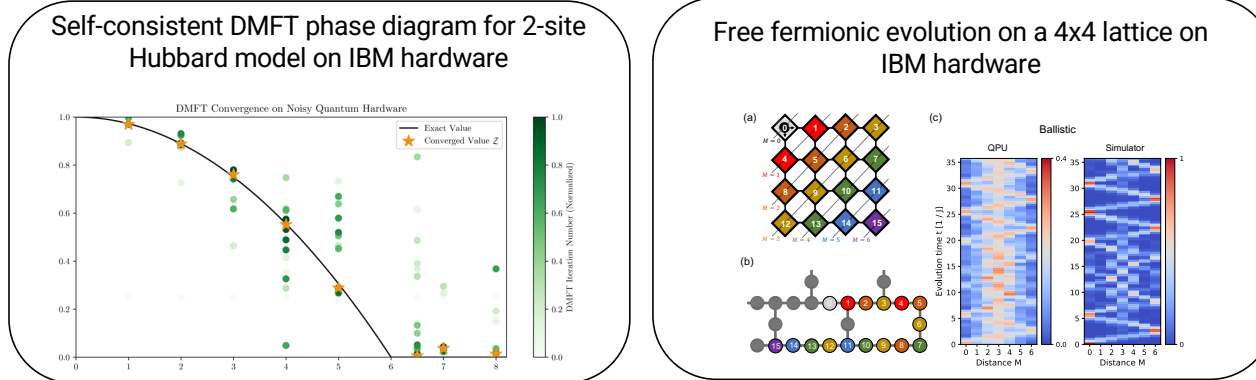
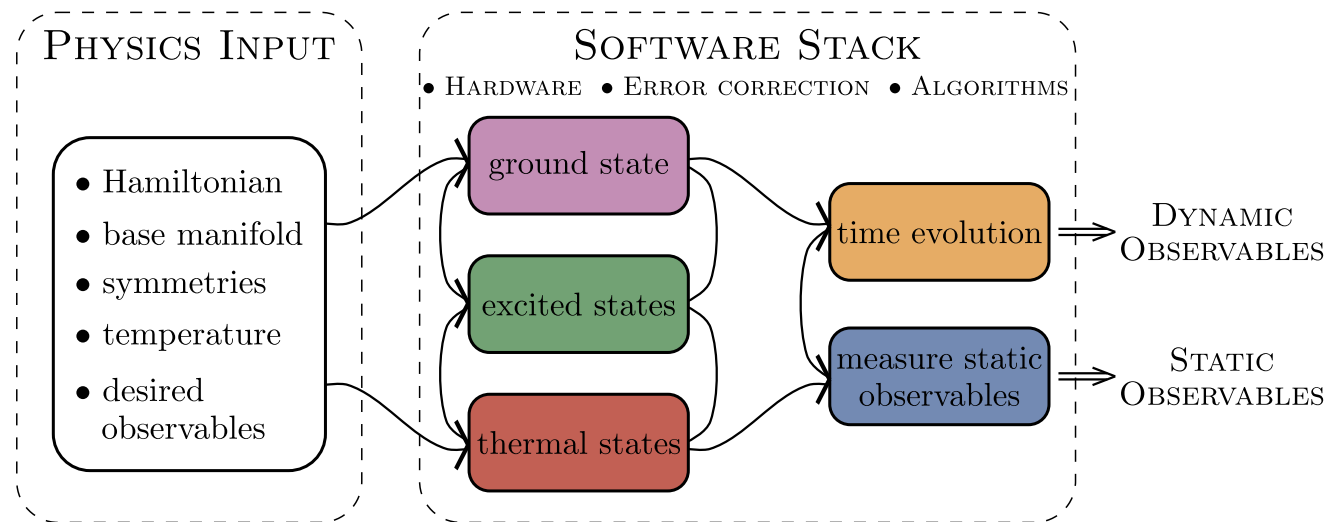
Phys. Rev. Lett. 93, 076401 (2004)



Johnston & Kemper, unpublished

Quantum Matter meets Quantum Computing

<https://go.ncsu.edu/kemper-lab>



- Experimental relevance:
Measuring correlation functions
- Measuring exact integer Chern numbers for topological states
- Driven/dissipative systems and fixed points (1000 Trotter steps)
- Exact time evolution via Lie algebraic decomposition and compression
- Thermodynamics via Lee-Yang Zeros
- Physics-Informed Subspace Expansions

Q: What do you do with a quantum state once you've prepared one?

Ising Model

794

Brazilian Journal of Physics, vol. 30, no. 4, December, 2000

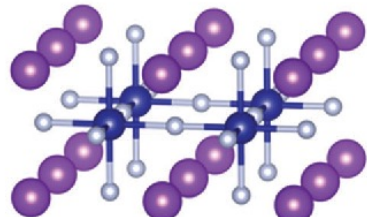
The Ising Model and Real Magnetic Materials

W. P. Wolf

*Yale University, Department of Applied Physics,
P.O. Box 208284, New Haven, Connecticut 06520-8284, U.S.A.*

Received on 3 August, 2000

The factors that make certain magnetic materials behave similarly to corresponding Ising models are reviewed. Examples of extensively studied materials include $\text{Dy}(\text{C}_2\text{H}_5\text{SO}_4)_3 \cdot 9\text{H}_2\text{O}$ (DyES), $\text{Dy}_3\text{Al}_5\text{O}_{12}$ (DyAlG), DyPO_4 , $\text{Dy}_2\text{Ti}_2\text{O}_7$, LiTbF_4 , K_2CoF_4 , and Rb_2CoF_4 . Various comparisons between theory and experiment for these materials are examined. The agreement is found to be generally very good, even when there are clear differences between the ideal Ising model and the real materials. In a number of experiments behavior has been observed that requires extensions of the usual Ising model. These include the effects of long range magnetic dipole interactions, competing interaction effects in field-induced phase transitions, induced staggered field effects and frustration effects, and dynamic effects. The results show that the Ising model and real magnetic materials have provided an unusually rich and productive field for the interaction between theory and experiment over the past 40 years.



[10.1039/c6cp02362b](https://doi.org/10.1039/c6cp02362b)

Heisenberg model

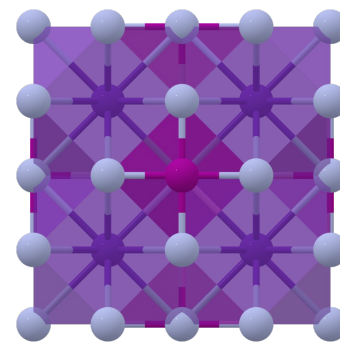
PHYSICAL REVIEW B

covering condensed matter and materials physics

Highlights Recent Accepted Collections Authors Referees Search Press

Critical behavior of the three-dimensional Heisenberg antiferromagnet RbMnF_3

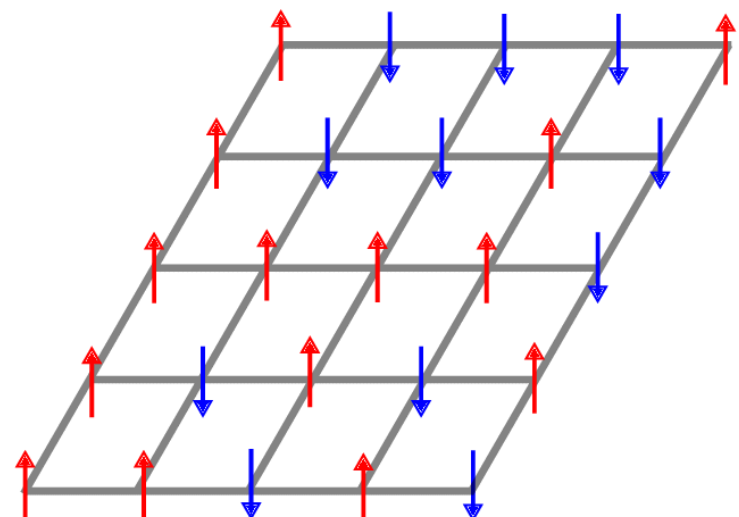
R. Coldea, R. A. Cowley, T. G. Perring, D. F. McMorrow, and B. Roessli
Phys. Rev. B **57**, 5281 – Published 1 March 1998



Materials project

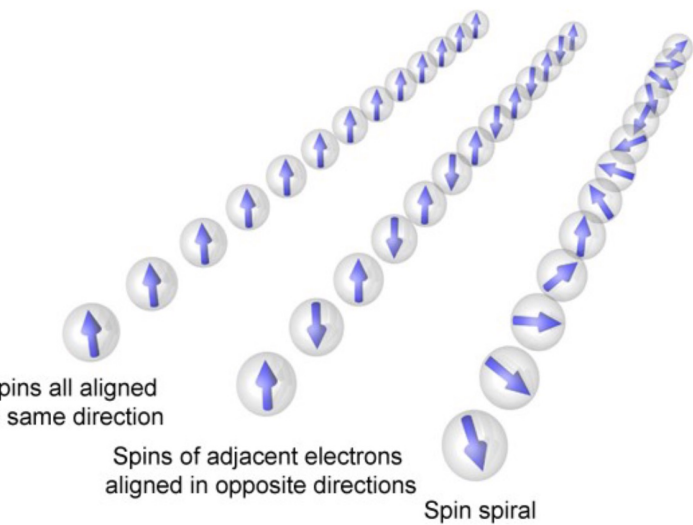
Ising Model

$$\mathcal{H} = -J \sum_i \sigma_i^z \sigma_{i+1}^z + h_x \sum_i \sigma_i^x$$



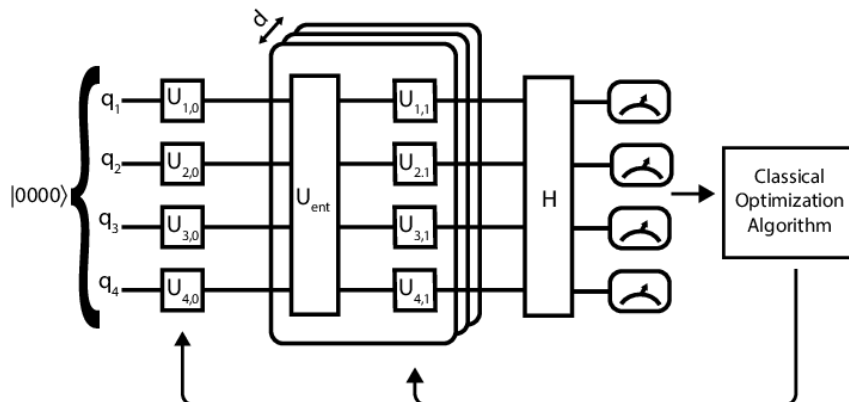
Heisenberg model

$$\mathcal{H} = -J \sum_i \vec{\sigma}_i \cdot \vec{\sigma}_{i+1} + h_x \sum_i \sigma_i^x$$



Ising Model

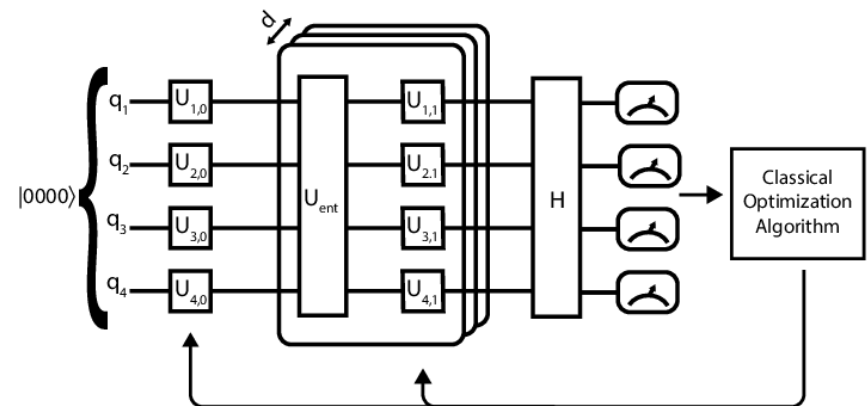
$$\mathcal{H} = -J \sum_i \sigma_i^z \sigma_{i+1}^z + h_x \sum_i \sigma_i^x$$



[Optimization of the Variational Quantum Eigensolver for Quantum Chemistry Applications](#)

Heisenberg model

$$\mathcal{H} = -J \sum_i \vec{\sigma}_i \cdot \vec{\sigma}_{i+1} + h_x \sum_i \sigma_i^x$$



Ising Model

$$\mathcal{H} = -J \sum_i \sigma_i^z \sigma_{i+1}^z + h_x \sum_i \sigma_i^x$$

Ferromagnetic



Antiferromagnetic



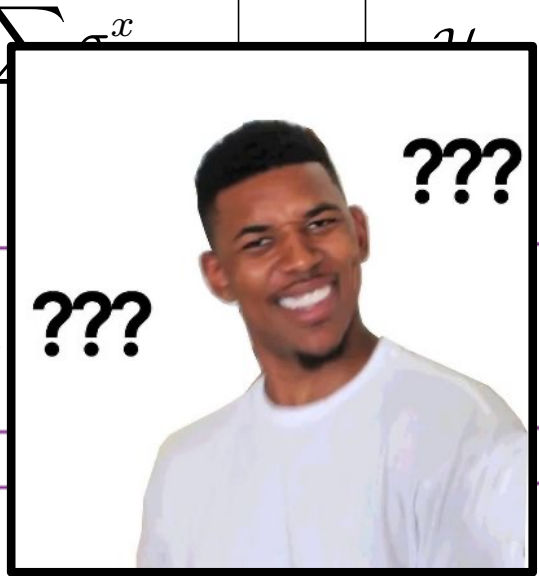
Heisenberg model

$$-J \sum_i \vec{\sigma}_i \cdot \vec{\sigma}_{i+1} + h_x \sum_i \sigma_i^x$$

Ferromagnetic



Antiferromagnetic



Ising Model

794

Brazilian Journal of Physics, vol. 30, no. 4, December, 2000

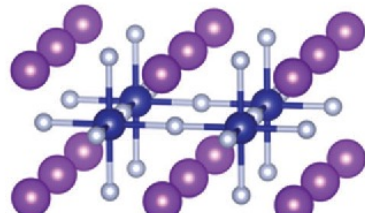
The Ising Model and Real Magnetic M

W. P. Wolf

*Yale University, Department of Applied Physics,
P.O. Box 208284, New Haven, Connecticut 06520-8284, U.S.A.*

Received on 3 August, 2000

The factors that make certain magnetic materials behave similarly to corresponding ideal Ising models are reviewed. Examples of extensively studied materials include Dy(C₂H₅SO₄)₂, Dy₃Al₅O₁₂ (DyAlG), DyPO₄, Dy₂Ti₂O₇, LiTbF₄, K₂CoF₄, and Rb₂CoF₄. Various differences between theory and experiment for these materials are examined. The agreement is generally very good, even when there are clear differences between the ideal Ising model and the real materials. In a number of experiments behavior has been observed that requires extensions of the usual Ising model. These include the effects of long range magnetic dipole interactions, interaction effects in field-induced phase transitions, induced staggered field effects, and dynamic effects. The results show that the Ising model and real magnetic materials provided an unusually rich and productive field for the interaction between theory and experiment over the past 40 years.



[10.1039/c6cp02362b](https://doi.org/10.1039/c6cp02362b)

Heisenberg model

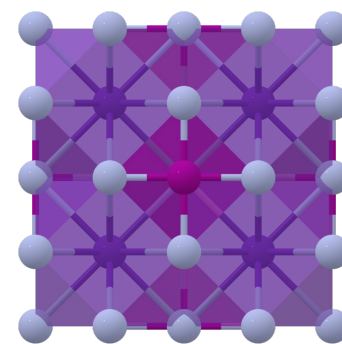
PHYSICAL REVIEW B

condensed matter and materials physics

Recent Accepted Collections Authors Referees Search Press

Physical behavior of the three-dimensional Heisenberg ferromagnet RbMnF₃

J. R. Cowley, T. G. Perring, D. F. McMorrow, and B. Roessli
Phys. Rev. B **57**, 5281 – Published 1 March 1998



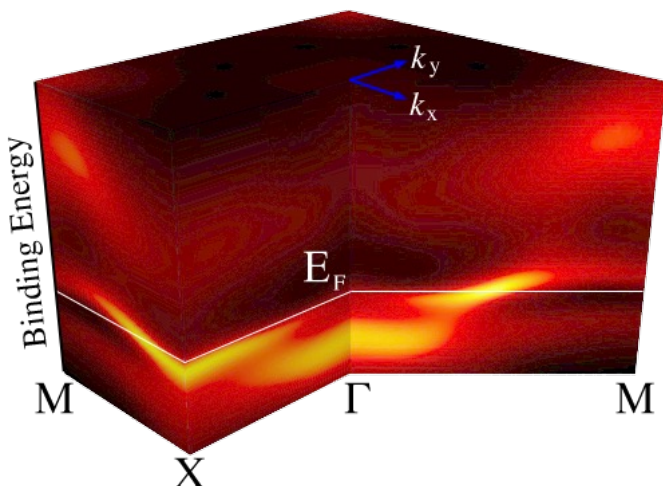
Materials project

Q: What do you do with a quantum state once you've prepared one?

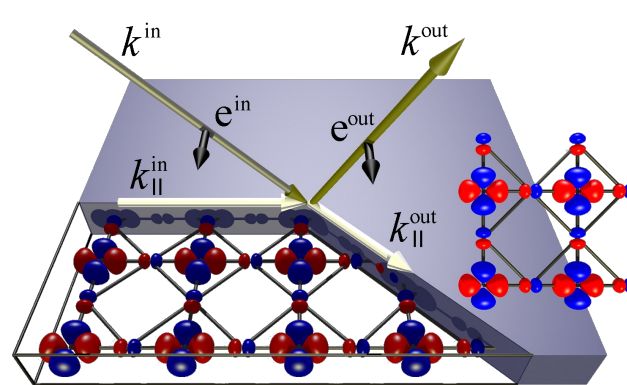
A: You measure its excitations.

Measuring Excitations

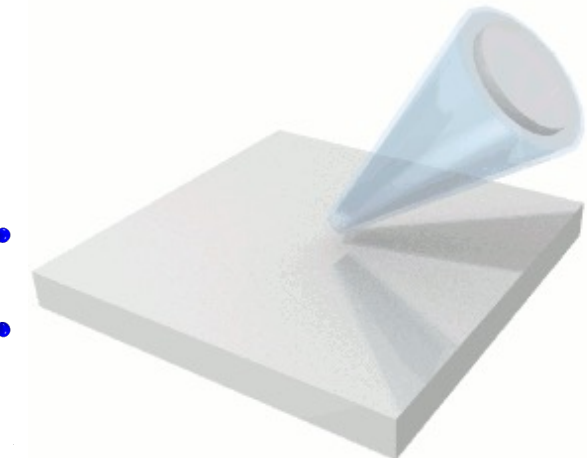
Figures courtesy of
Devereaux group



Angle-resolved Photoemission
(ARPES)

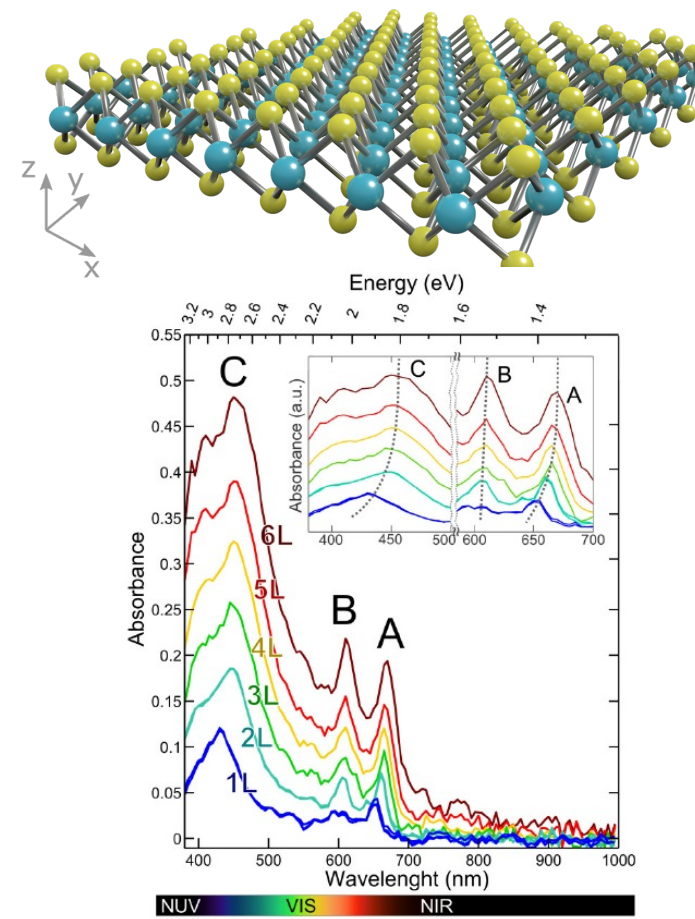
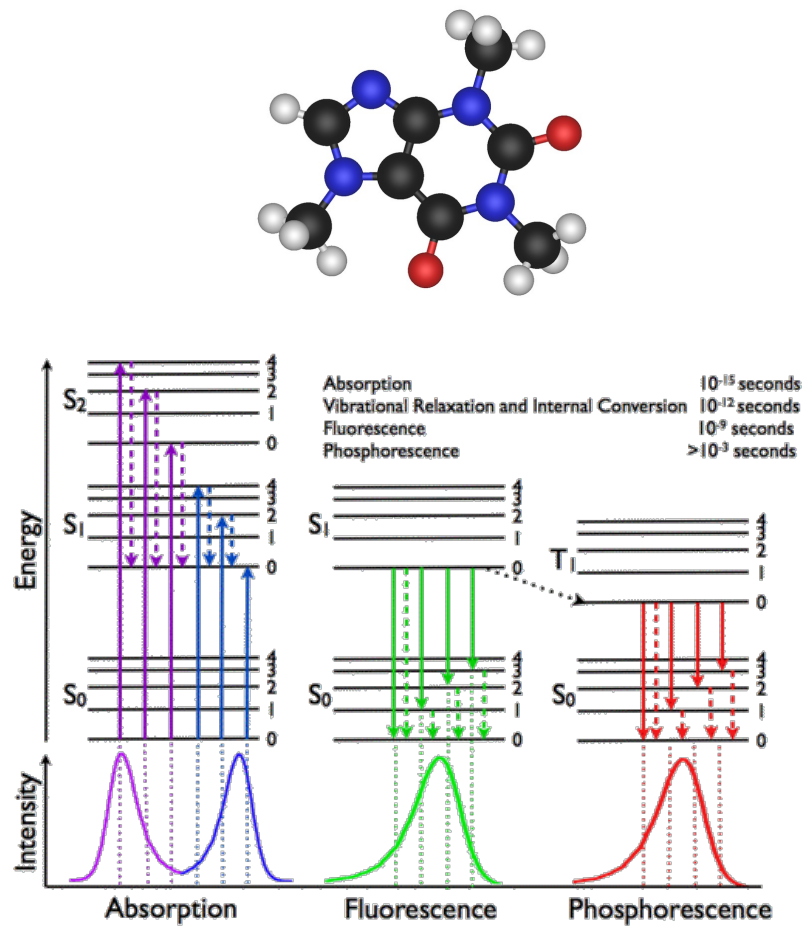


Resonant Inelastic X-Ray
Scattering



Time-resolved ARPES

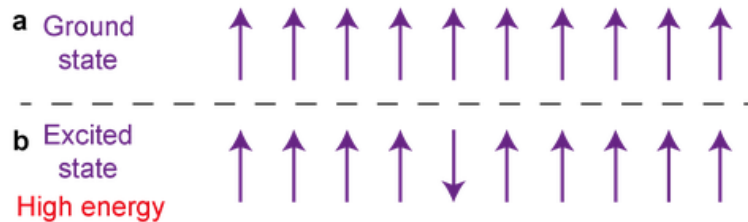
Measuring Excitations



Measuring Excitations

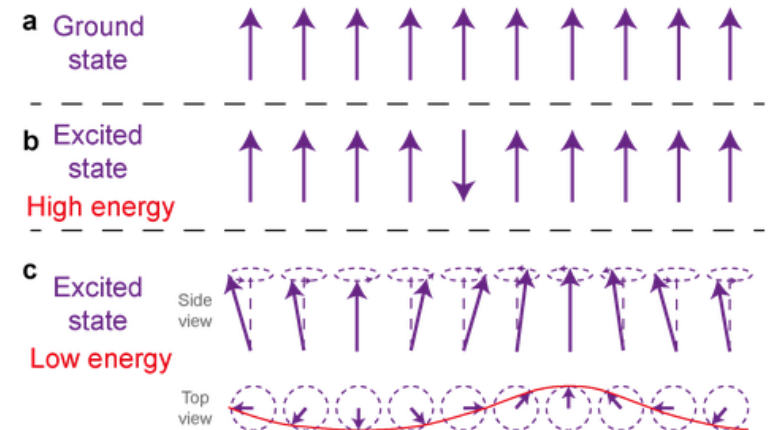
Ising Model

$$\mathcal{H} = -J \sum_i \sigma_i^z \sigma_{i+1}^z + h_x \sum_i \sigma_i^x$$



Heisenberg model

$$\mathcal{H} = -J \sum_i \vec{\sigma}_i \cdot \vec{\sigma}_{i+1} + h_x \sum_i \sigma_i^x$$



Measuring Excitations – Response functions

Schrödinger Picture

$$i\partial_t |\psi(t)\rangle = H|\psi(t)\rangle$$

Heisenberg Picture

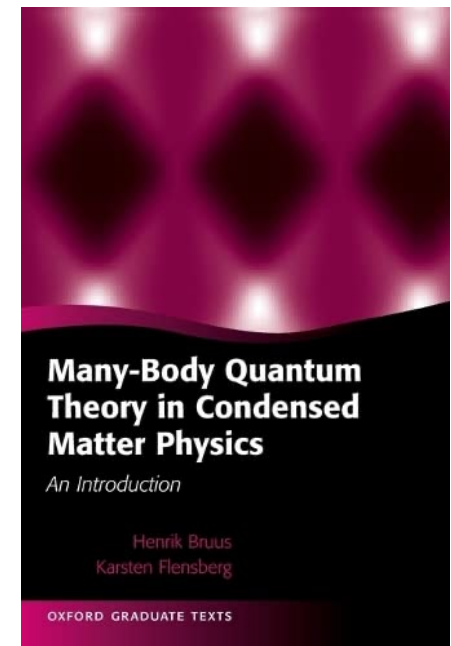
$$i\partial_t \mathcal{O}(t) = [\mathcal{O}(t), H(t)]$$

Interaction Picture

$$H = H_0 + V(t)$$

$$i\partial_t |\psi(t)\rangle = V(t)|\psi(t)\rangle$$

$$i\partial_t \mathcal{O}(t) = [\mathcal{O}(t), H_0]$$



Some Mathematics...

The time evolution operator satisfies

$$i\partial_t U(t) = V(t)U(t)$$

Which is formally solved by

$$U(t) = \mathcal{T} \exp \left(-i \int_{-\infty}^t V(\bar{t}) d\bar{t} \right)$$

Or approximately(for small V) by

$$U(t) \approx 1 - i \int_{-\infty}^t V(\bar{t}) d\bar{t}$$

Thus the wave function is given by

$$|\psi(t)\rangle \approx |\psi_0\rangle - i \int_{-\infty}^t V(\bar{t}) |\psi_0\rangle d\bar{t}$$

We now pick an operator **A** to evaluate

$$\langle \psi(t) | \mathbf{A}(t) | \psi(t) \rangle = \langle \psi_0 | \mathbf{A}(t) | \psi_0 \rangle = \\ -i \int_{-\infty}^t \langle \psi_0 | [\mathbf{A}(t), \mathbf{V}(\bar{t})] | \psi_0 \rangle d\bar{t}$$

Putting the time dependence outside via $\mathbf{V}(t) = h(t)\mathbf{B}$

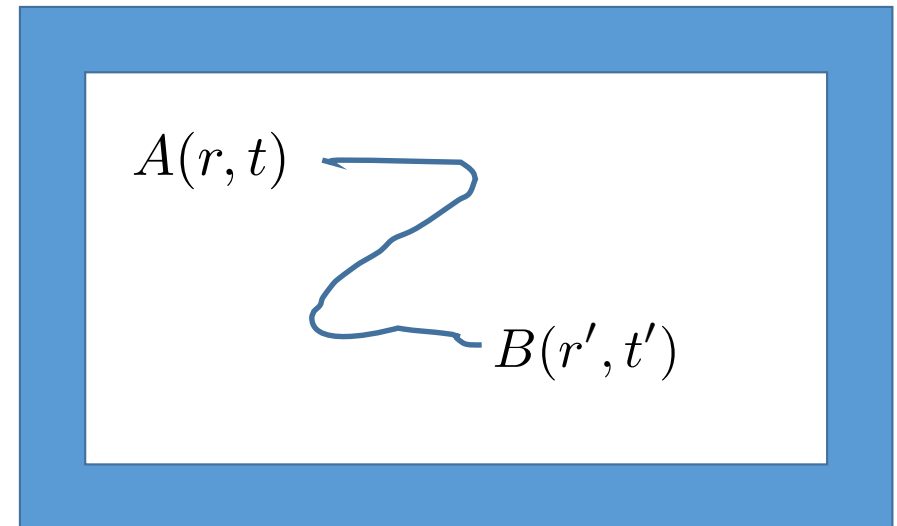
$$\delta A(t) = -i \int_{-\infty}^t \langle [\mathbf{A}(t), \mathbf{B}] \rangle h(\bar{t}) d\bar{t}$$

$$\delta A(t) = \int_{\infty}^{\infty} \chi^R(t, \bar{t}) h(\bar{t}) d\bar{t}$$

Low-energy excitations: correlation functions

$$\langle A(r, t)B(r', t') \rangle$$

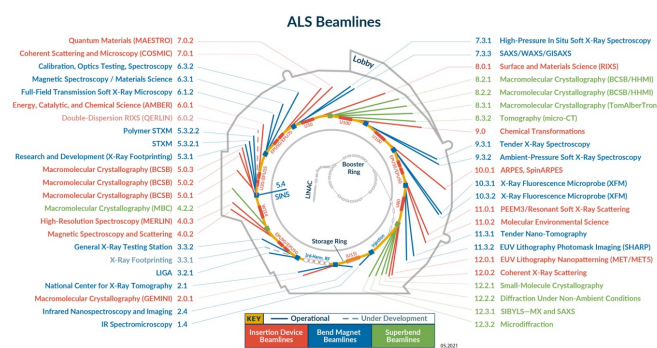
Given some (observable) operator B at (r',t'), what is the likelihood of some (observable) operator A at (r,t)?



$$\delta A(t) = -i \int_{-\infty}^t \langle [\mathbf{A}(t), \mathbf{B}] \rangle h(\bar{t}) d\bar{t} = \int_{-\infty}^{\infty} \chi^R(t, \bar{t}) h(\bar{t}) d\bar{t}$$

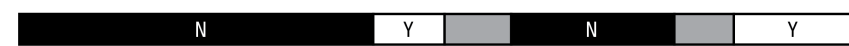
Experiment	Applied field B	Measured operator A	Correlation function
AC Conductivity	Electric field	Current	[j,j]
Neutron Scattering	Spin flip	Spin flip/Z	[Sx,Sx] etc
Magnetic Susceptibility	Magnetic	Spin	[Sz,Sz], [S+,S-]
Photoemission spectroscopy	Particle removal	Particles at detector	[c+,c]
Light absorption	p.A	j	A.[p, j]
Light scattering	p.A	p.A	A1.[p1, p2].A2

$$\delta A(t) = -i \int_{-\infty}^t \langle [\mathbf{A}(t), \mathbf{B}] \rangle h(\bar{t}) d\bar{t} = \int_{\infty}^{\infty} \chi^R(t, \bar{t}) h(\bar{t}) d\bar{t}$$



THE ELECTROMAGNETIC SPECTRUM

P e n e t r a t e E a r t h ' s A t m o s p h e r e



Radiation Type	Gamma Ray	X-ray	Ultraviolet	Visible	Infrared	Microwave	Radio
Wavelength (m)	10^{-12}	10^{-10}	10^{-8}	5×10^{-6}	10^{-5}	10^{-1}	10^3



About the Size of

Short wavelength
High energy
High frequency

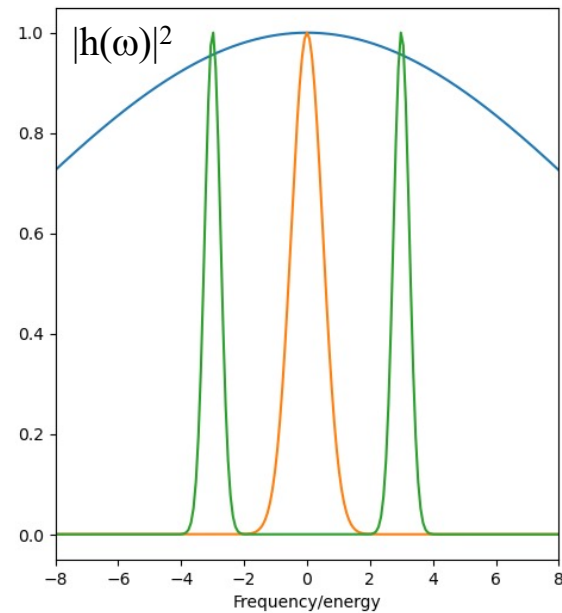
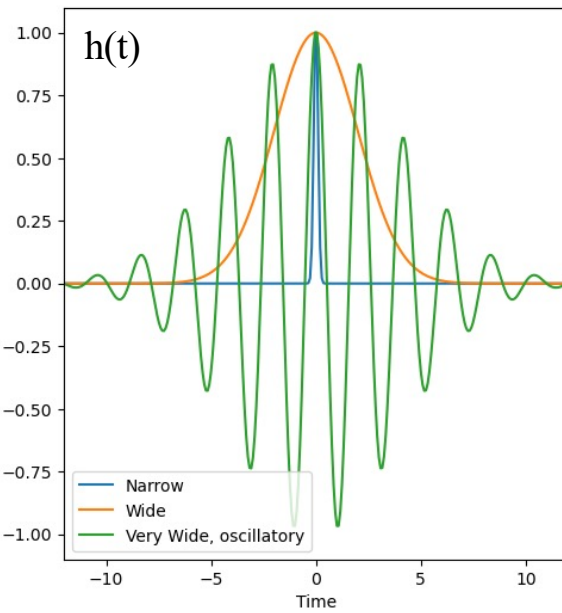


Long wavelength
Low energy
Low frequency

The Electromagnetic Spectrum. Image Credit: NASA

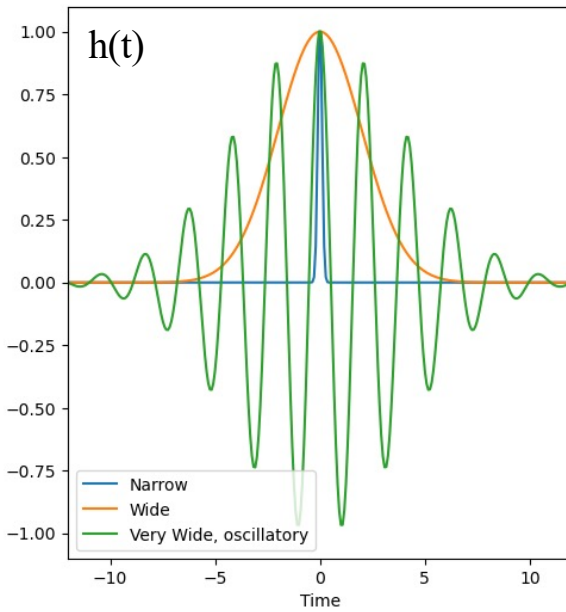
$$\delta A(t) = -i \int_{-\infty}^t \langle [\mathbf{A}(t), \mathbf{B}] \rangle h(\bar{t}) d\bar{t} = \int_{-\infty}^{\infty} \chi^R(t, \bar{t}) h(\bar{t}) d\bar{t}$$

$h(t)$ encodes the energy range/resolution



$$\delta A(t) = -i \int_{-\infty}^t \langle [\mathbf{A}(t), \mathbf{B}] \rangle h(\bar{t}) d\bar{t} = \int_{-\infty}^{\infty} \chi^R(t, \bar{t}) h(\bar{t}) d\bar{t}$$

$h(t)$ encodes the energy range/resolution

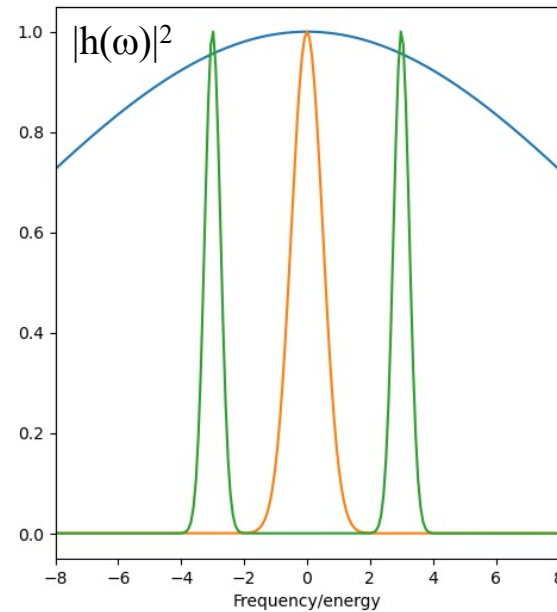


\mathbf{B} can be used for spatial encoding

$$\mathbf{B} = \frac{1}{N} \sum_i \sigma_i^z$$

vs

$$\mathbf{B} = \frac{1}{N} \sum_i (-1)^i \sigma_i^z$$

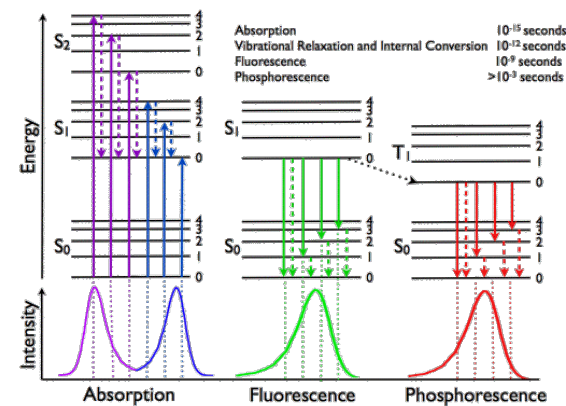


Some More Mathematics...

The task is to calculate

$$\chi(t) := -i\theta(t)\langle\psi_0|\mathbf{A}(t)\mathbf{B}|\psi_0\rangle$$

$$\chi(\omega) = \sum_j \frac{\langle\psi_0|\mathbf{A}|j\rangle\langle j|\mathbf{B}|\psi_0\rangle}{\omega - E_j + E_0 + i\varepsilon}$$

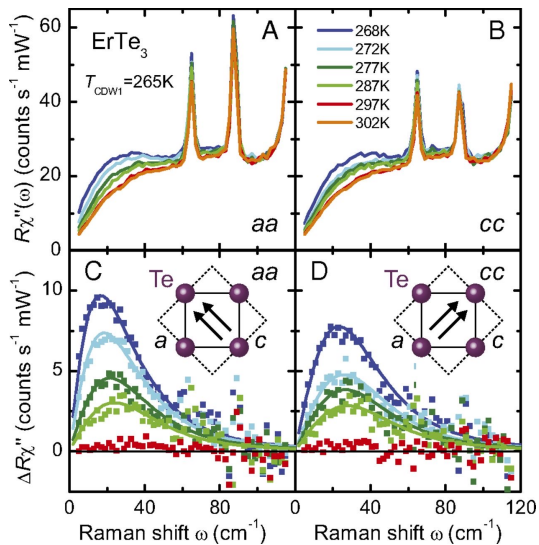


Some More Mathematics...

The task is to calculate

$$\chi(r, r', t) := -i\theta(t)\langle\psi_0|\mathbf{A}(r, t)\mathbf{B}(r')|\psi_0\rangle$$

$$\chi(q, \omega) = \int d(r - r') e^{-iq(r-r')} \frac{\langle\psi_0|\mathbf{A}(r)|j\rangle\langle j|\mathbf{B}(r')|\psi_0\rangle}{\omega - E_j + E_0 + i\varepsilon}$$



RESEARCH ARTICLE | PHYSICAL SCIENCES | [DOI](#)

f t in e

Alternative route to charge density wave formation in multiband systems

Hans-Martin Eiter, Michela Lavagnini, Rudi Hackl [+6](#), and Leonardo Degiorgi [Authors Info & Affiliations](#)

Edited by M. Brian Maple, University of California at San Diego, La Jolla, CA, and approved November 15, 2012 (received for review August 24, 2012)

December 17, 2012 | 110 (1) 64-69 | <https://doi.org/10.1073/pnas.1214745110>

RESEARCH ARTICLE | APPLIED PHYSICAL SCIENCES | [DOI](#)

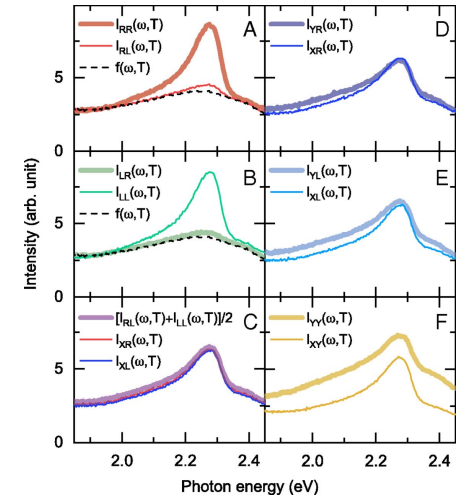
f t in e

Observation of chiral surface excitons in a topological insulator Bi_2Se_3

H.-H. Kung [+6](#), A. P. Goyal, D. L. Maslov [+4](#), and G. Blumberg [Authors Info & Affiliations](#)

Edited by Angel Rubio, Max Planck Institute for the Structure and Dynamics of Matter, Hamburg, Germany, and approved January 22, 2019 (received for review August 5, 2018)

February 20, 2019 | 116 (10) 4006-4011 | <https://doi.org/10.1073/pnas.1813514116>



Quantum Algorithm(s) for χ

Quantum Algorithm(s) for χ

APPROACH 1: Stick with the many–body textbook

$$\chi(\omega) \langle \psi_0 | \sum_j \frac{\langle \psi_0 | \mathbf{A} | j \rangle \langle j | \mathbf{B} | \psi_0 \rangle}{\omega - E_j + i\epsilon} | \psi_0 \rangle$$

APPROACH 2: Go back to our roots

$$\chi(t) = e^{iE_0 t} \langle \psi_0 | \mathbf{A} e^{-i\mathbf{H}_0 t} \mathbf{B} | \psi_0 \rangle$$

Quantum Algorithm(s) for χ

$$\chi(t) = e^{iE_0 t} \langle \psi_0 | \mathbf{A} e^{-i\mathbf{H}_0 t} \mathbf{B} | \psi_0 \rangle$$

Interfere with ground state Complete expectation value Time evolve Apply excitation B Apply excitation A

PHYSICAL REVIEW A, VOLUME 65, 042323

PRL 113, 020505 (2014)

PHYSICAL REVIEW LETTERS

week ending
11 JULY 2014

Simulating physical phenomena by quantum networks

R. Somma, G. Ortiz, J. E. Gubernatis, E. Knill, and R. Laflamme

Los Alamos National Laboratory, Los Alamos, New Mexico 87545

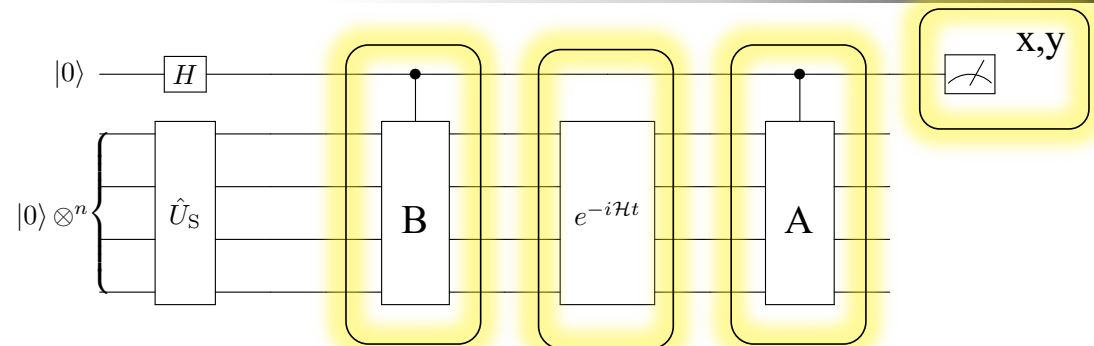
(Received 12 September 2001; published 9 April 2002)

Efficient Quantum Algorithm for Computing n -time Correlation Functions

J. S. Pedernales,¹ R. Di Candia,¹ I. L. Egusquiza,² J. Casanova,¹ and E. Solano^{1,3}¹Department of Physical Chemistry, University of the Basque Country UPV/EHU, Apartado 644, 48080 Bilbao, Spain²Department of Theoretical Physics and History of Science, University of the Basque Country UPV/EHU, Apartado 644, 48080 Bilbao, Spain³IKERBASQUE, Basque Foundation for Science, Alameda Urquijo 36, 48011 Bilbao, Spain

(Received 20 January 2014; revised manuscript received 30 April 2014; published 10 July 2014)

Quantum Algorithm(s) for χ

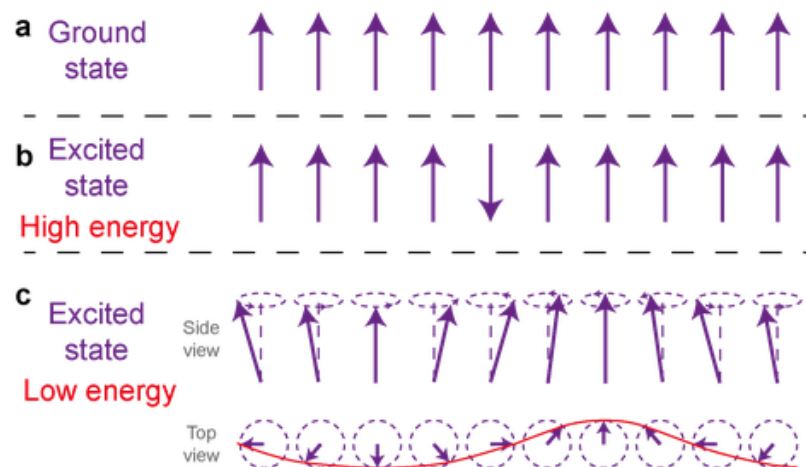


$$(|0\rangle + |1\rangle) |\psi_0\rangle$$

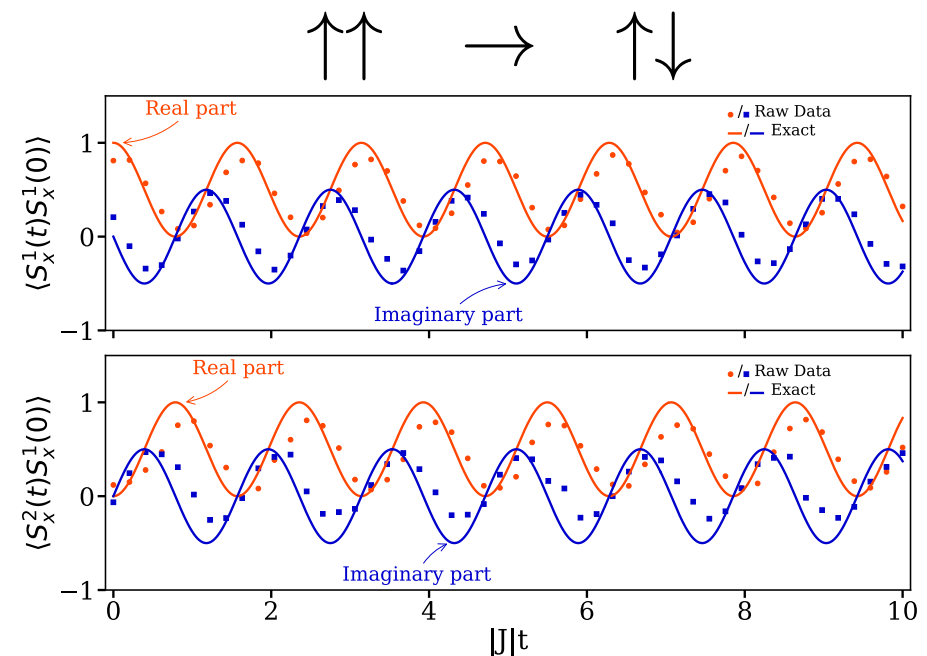
$$P(0) = \frac{1}{2} [1 + \operatorname{Re} e^{iE_0 t} \langle \psi_0 | \mathbf{A} e^{-i\mathbf{H}_0 t} \mathbf{B} | \psi_0 \rangle]$$

Low-energy excitations: 2-site magnons

Spin-spin correlation function for periodic Heisenberg model: Magnons!



$$\hat{H} = 2SJ \sum_k (1 - \cos(k)) \hat{c}_k^\dagger \hat{c}_k$$

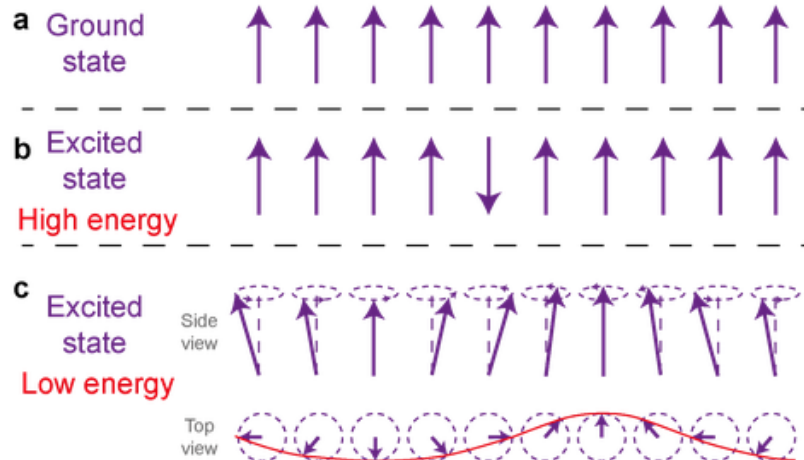


Data from *ibmq_tokyo*

[10.1103/PhysRevB.101.014411](https://doi.org/10.1103/PhysRevB.101.014411)

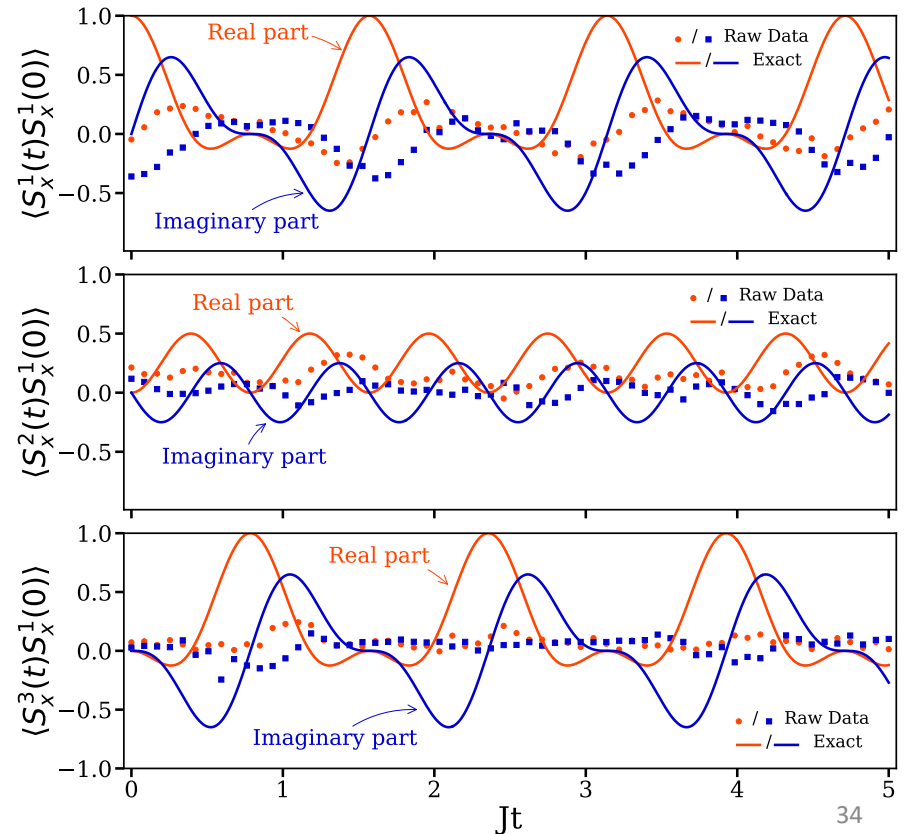
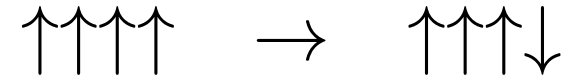
Low-energy excitations: 4-site magnons

Spin-spin correlation function for periodic Heisenberg model

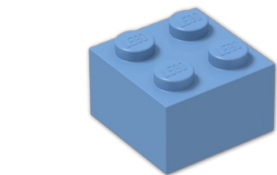
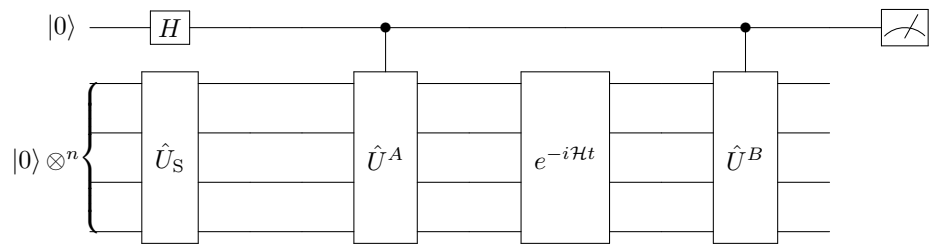


$$\hat{H} = 2SJ \sum_k (1 - \cos(k)) \hat{c}_k^\dagger \hat{c}_k$$

Data from *ibmq_tokyo*



Quantum Compiling



Single Qubit Gates

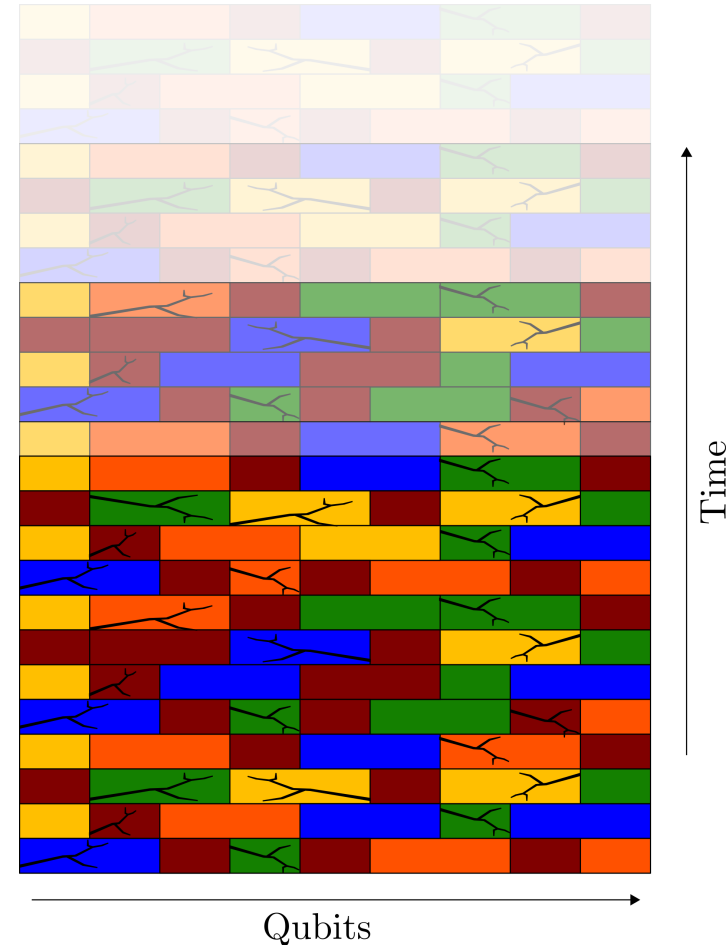
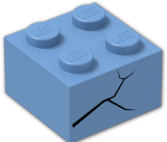
+



Two Qubit Gate

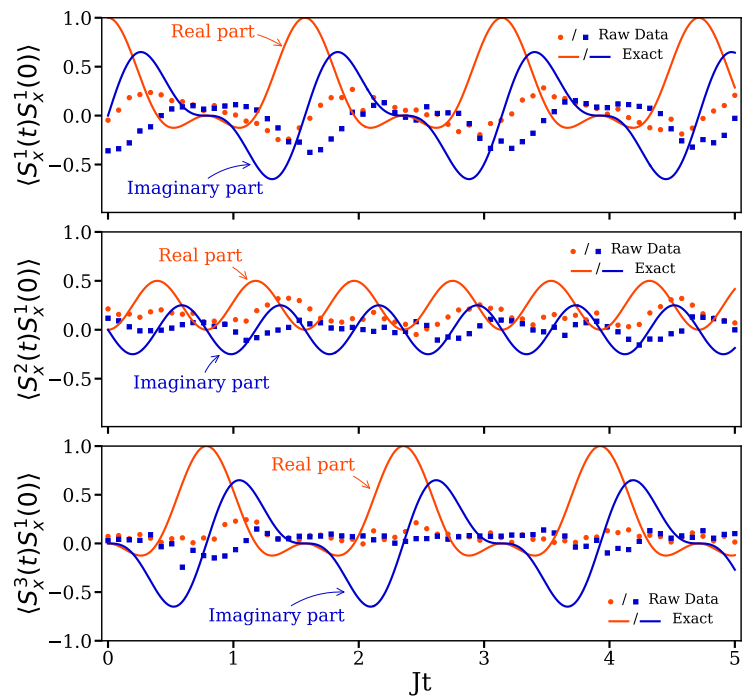
= Anything!*

*Actual Gates

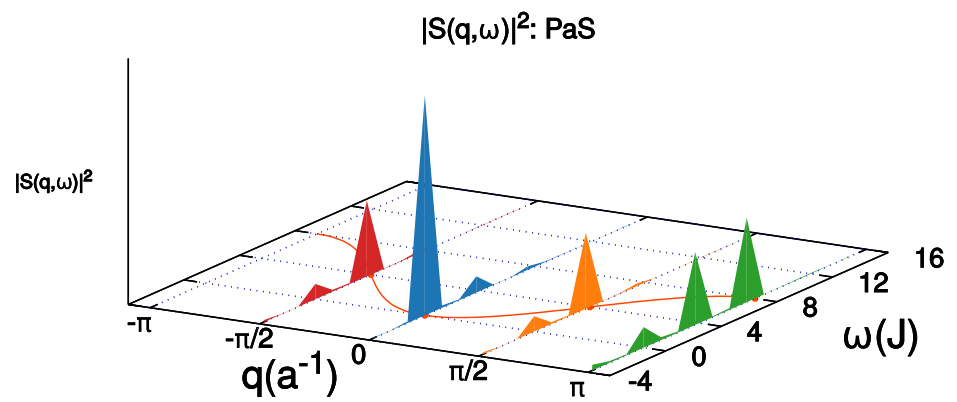


Low-energy excitations: 4-site magnons

Spin-spin correlation function for periodic Heisenberg model: Magnons!

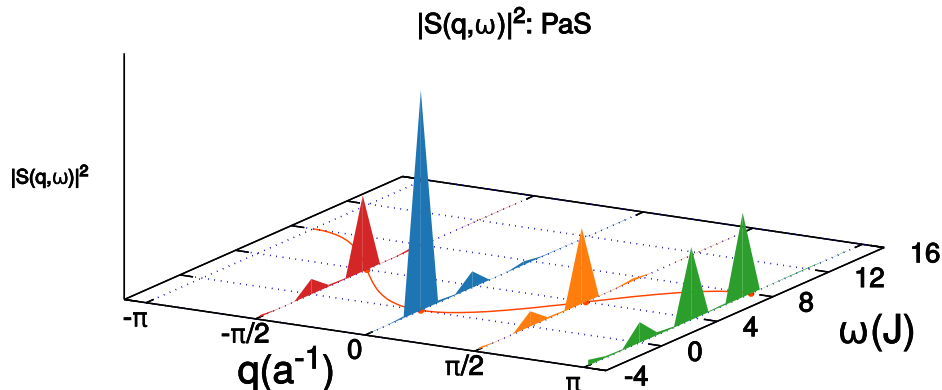


$$\begin{array}{c} \text{FT} \\ \xrightarrow{\hspace{1cm}} \\ t \rightarrow \omega \\ r \rightarrow k \end{array}$$



Low-energy excitations: 4-site magnons

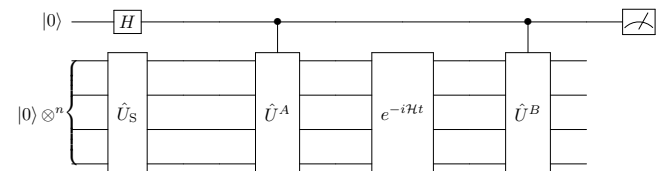
Spin-spin correlation function for periodic Heisenberg model: Magnons!



This works!

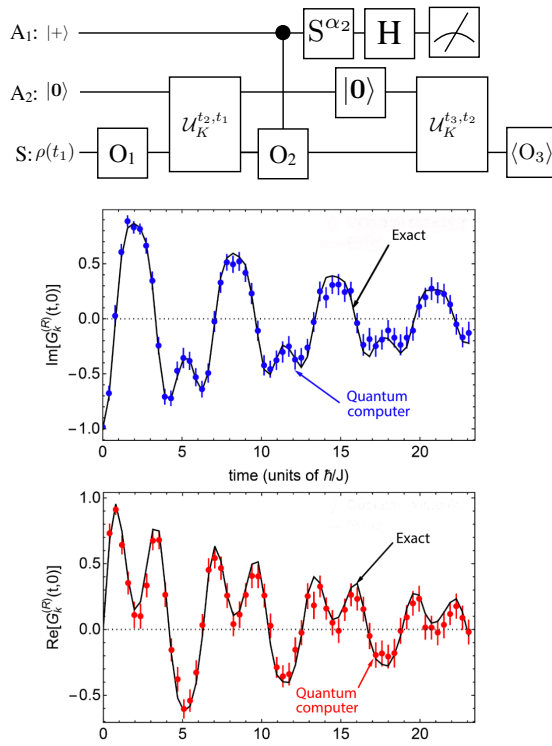
But:

- Need an ancilla with long coherence
- A and B need to be unitary & controlled
- More complex A,B need post-processing



[10.1103/PhysRevB.101.014411](https://doi.org/10.1103/PhysRevB.101.014411)

(A few) Quantum Algorithm(s) for χ



(Anti-)Commutators, dissipative

L. Del Re, B. Rost, M. Foss-Feig, AFK, J.K. Freericks
2204.12400

1. Initial state preparation
2. Time evolution until time t_1
3. Weak coupling of ancilla and system site i .
4. Measuring the ancilla
5. Time evolution until time t_2
6. Projective measurement at site j
7. Correlating the measured outcomes

Anti-commutators

10.1103/PhysRevA.96.022127

PRL 111, 147205 (2013) PHYSICAL REVIEW LETTERS week ending 4 OCTOBER 2013

Probing Real-Space and Time-Resolved Correlation Functions with Many-Body Ramsey Interferometry

Michael Knap,^{1,2,*} Adrian Kantian,³ Thierry Giamarchi,³ Immanuel Bloch,^{4,5} Mikhail D. Lukin,¹ and Eugene Demler¹

¹Department of Physics, Harvard University, Cambridge, Massachusetts 02138, USA
²JTAMP, Harvard-Smithsonian Center for Astrophysics, Cambridge, Massachusetts 02138, USA
³DPMC-MaNEP, University of Geneva, 24 Quai Ernest-Ansermet CH-1211 Geneva, Switzerland
⁴Max-Planck-Institut für Quantenoptik, Hans-Kopfermann-Strasse 1, 85748 Garching, Germany
⁵Fakultät für Physik, Ludwig-Maximilians-Universität München, 80799 München, Germany
(Received 2 July 2013; revised manuscript received 18 September 2013; published 4 October 2013)

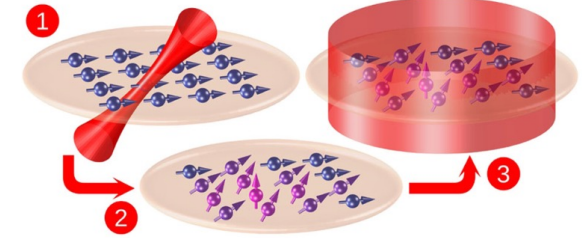
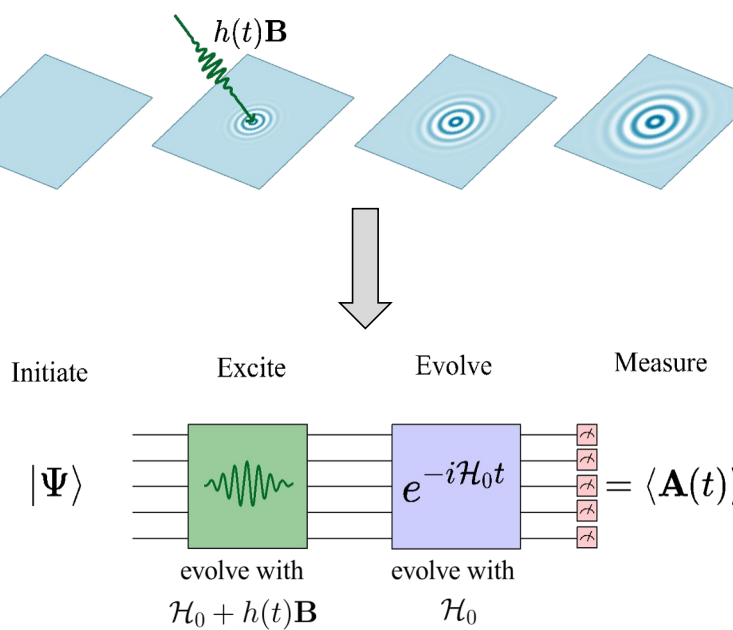
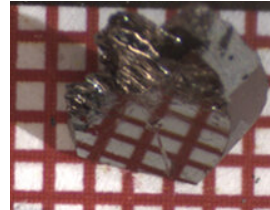


FIG. 1 (color online). Many-body Ramsey interferometry consists of the following steps: (1) A spin system prepared in its ground state is locally excited by $\pi/2$ rotation; (2) the system evolves in time; (3) a global $\pi/2$ rotation is applied, followed by the measurement of the spin state. This protocol provides the dynamic many-body Green's function.

Commutators

10.1103/PhysRevLett.111.147205

Linear Response



A linear response framework for simulating bosonic and fermionic correlation functions illustrated on quantum computers

Efekan Kökü¹, Heba A. Labib¹, J. K. Freericks² and A. F. Kemper^{1,*}

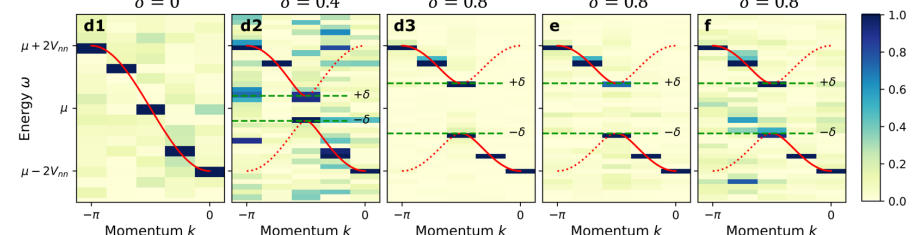
¹Department of Physics, North Carolina State University, Raleigh, North Carolina 27695, USA

²Department of Physics, Georgetown University, 37th and O Sts. NW, Washington, DC 20057 USA

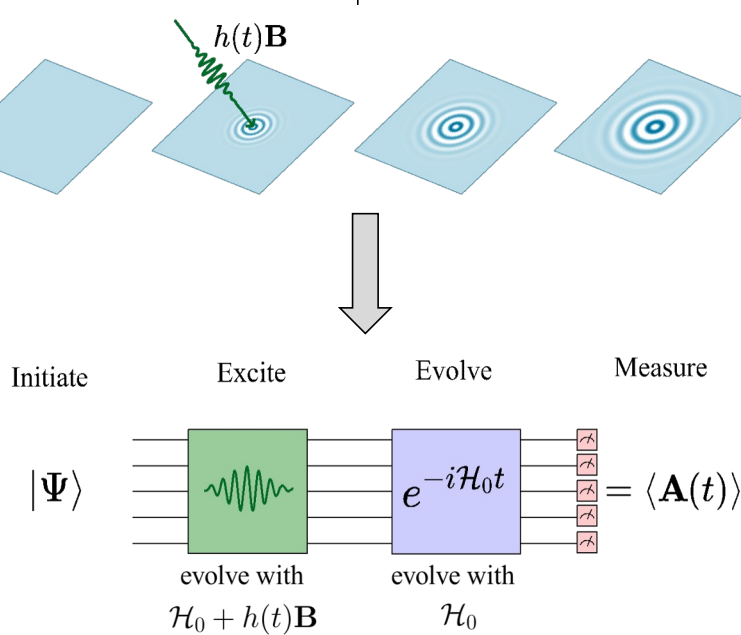
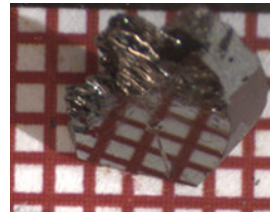
(Dated: February 22, 2023)

1. Make the excitation part of the quantum simulation
2. Post-process the data to get the response functions

$$\left. \frac{\delta A(t)}{\delta h(t')} \right|_{h=0} = -i\theta(t-t') \langle \psi_0 | [\mathbf{A}(t), \mathbf{B}(t')] | \psi_0 \rangle$$



Linear Response



A linear response framework for simulating bosonic and fermionic correlation functions illustrated on quantum computers

Efekan Kökcü ,¹ Heba A. Labib ,¹ J. K. Freericks ,² and A. F. Kemper ,^{1,*}

¹Department of Physics, North Carolina State University, Raleigh, North Carolina 27695, USA

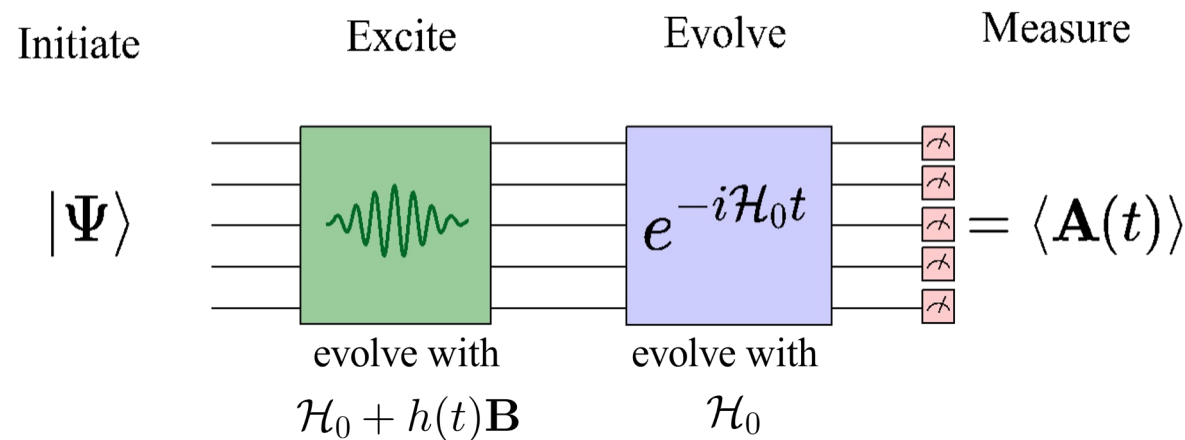
²Department of Physics, Georgetown University, 37th and O Sts. NW, Washington, DC 20057 USA

(Dated: February 22, 2023)

Benefits

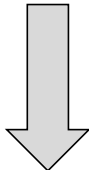
- Any operator A,B you desire (as long as it is Hermitian*)
- No ancillas/controlled operations needed
- Many correlation functions at the same time
- Less post-processing (less noise)
- Frequency/momentum selective

Even More Mathematics...



Even More Mathematics...

$$\begin{aligned}\langle \mathbf{A}(t) \rangle &= \langle \psi_0 | U(t)^\dagger \mathbf{A} U(t) | \psi_0 \rangle \\ &= \langle \psi_0 | \mathcal{T} e^{i \int_{-\infty}^t [\mathbf{H}_0 + \mathbf{B} h(\bar{t})] d\bar{t}} \mathbf{A} \mathcal{T} e^{-i \int_{-\infty}^t [\mathbf{H}_0 + \mathbf{B} h(\bar{t})] d\bar{t}} | \psi_0 \rangle\end{aligned}$$

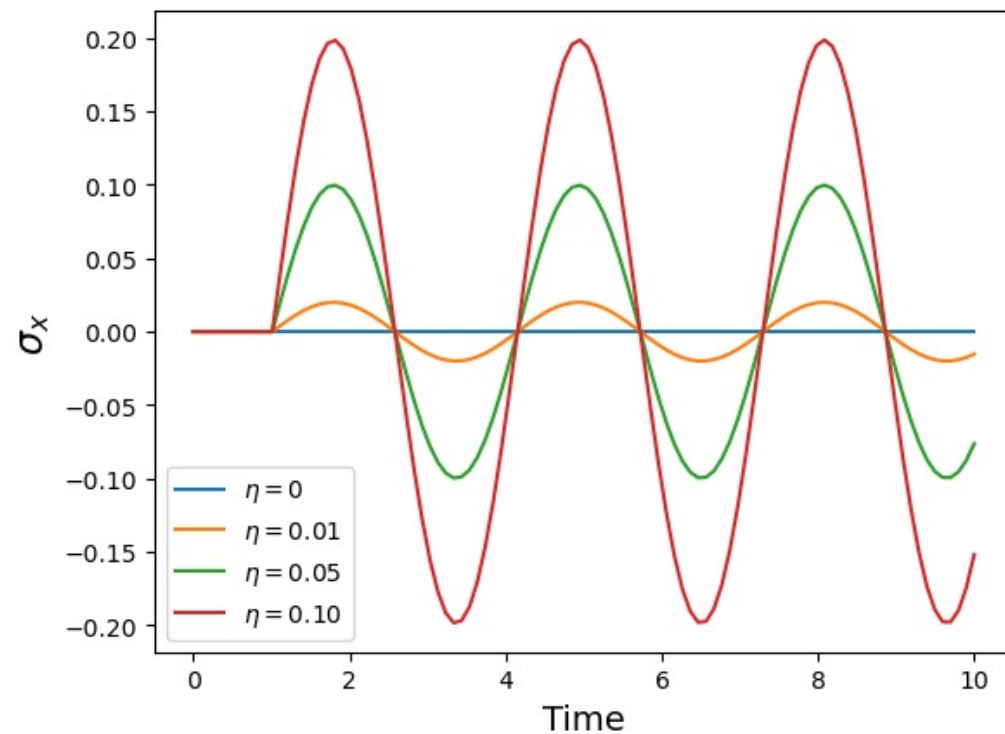
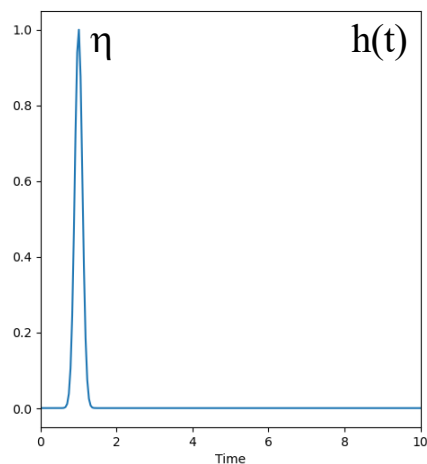


Linear Response

A simple example: single spin with energy level difference = 2

$$\mathbf{H}_0 = \sigma^z$$

$$\mathbf{A} = \mathbf{B} = \sigma^x$$

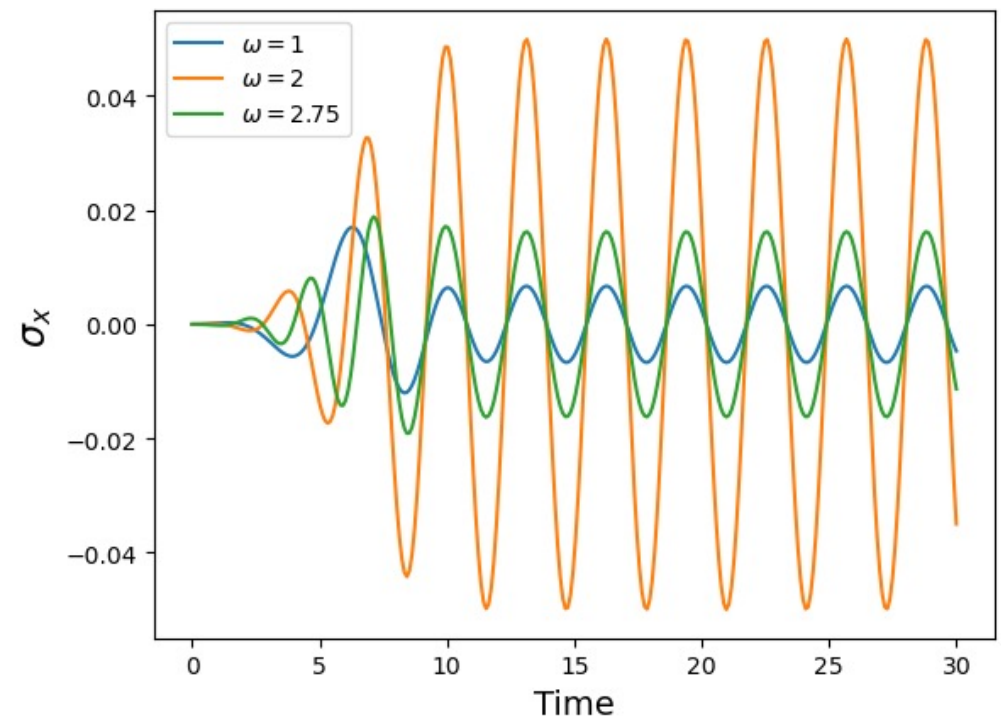
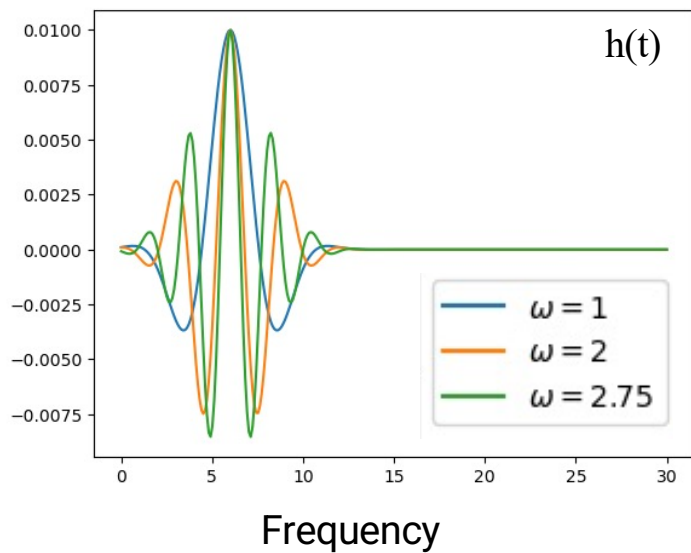


Linear Response

A simple example: single spin with energy level difference = 2

$$\mathbf{H}_0 = \sigma^z$$

$$\mathbf{A} = \mathbf{B} = \sigma^x$$

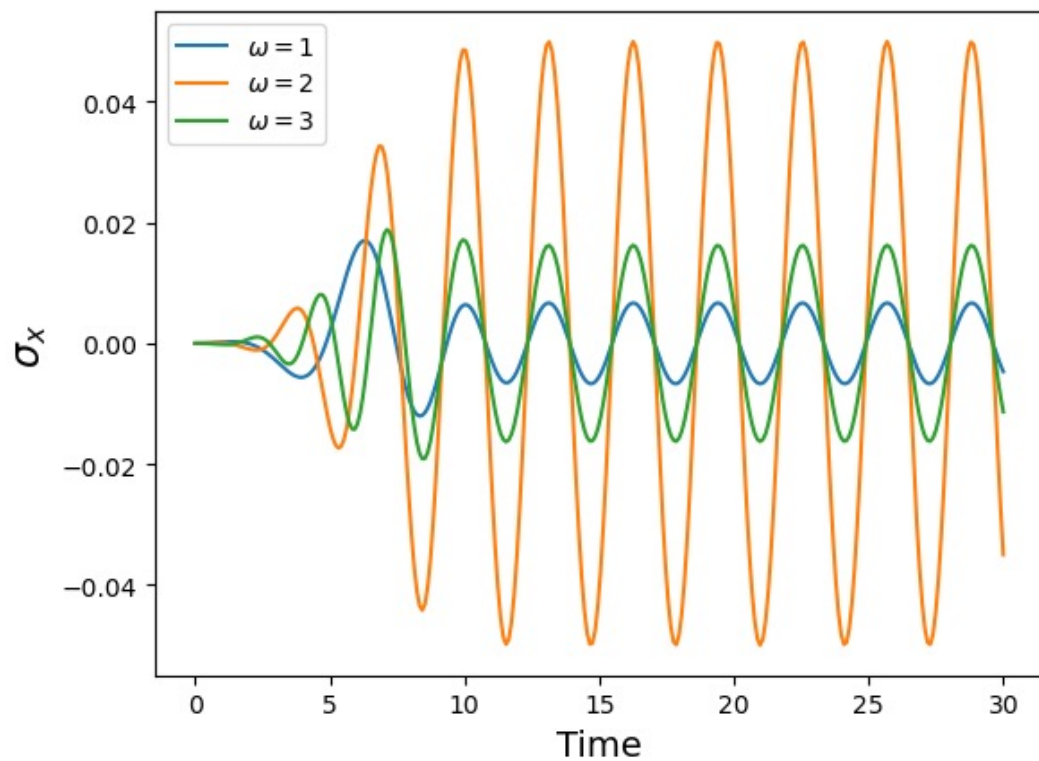
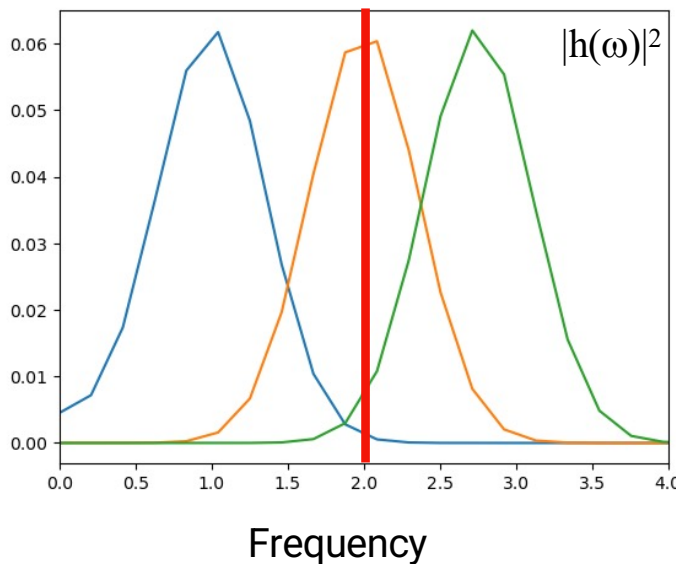


Linear Response

A simple example: single spin with energy level difference = 2

$$\mathbf{H}_0 = \sigma^z$$

$$\mathbf{A} = \mathbf{B} = \sigma^x$$



Bosonic (commutator) response functions:

- We calculate the functional derivative in the following way. For small values of $h(t)$:

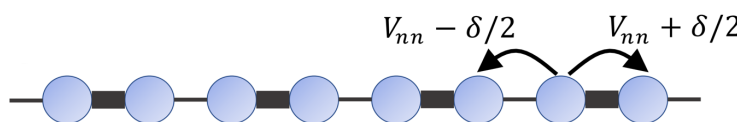
$$A(t) = \int dt' \chi^R(t - t') h(t') + \mathcal{O}(h^2)$$

- Fourier transformation leads to

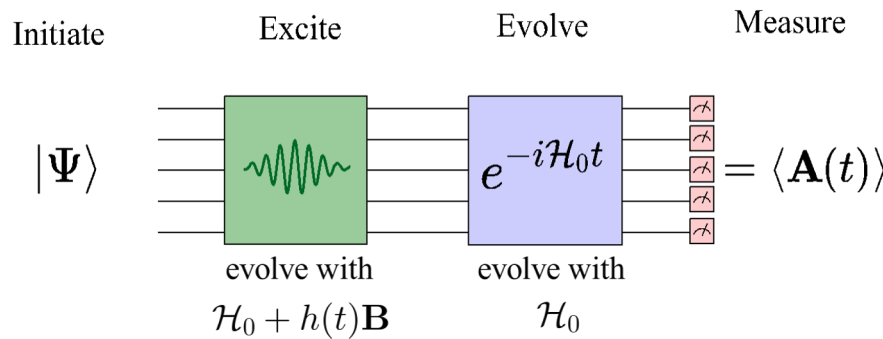
$$A(\omega) = \chi^R(\omega) h(\omega) + \mathcal{O}(h^2)$$

A Bosonic Correlation function: Polarizability

Su-Schrieffer-Heeger model for polyacetylene



$$\mathcal{H}_0 = - \sum_{\langle i,j \rangle} \left[V_{nn} + (-1)^i \delta/2 \right] c_i^\dagger c_j - \mu \sum_i c_i^\dagger c_i$$

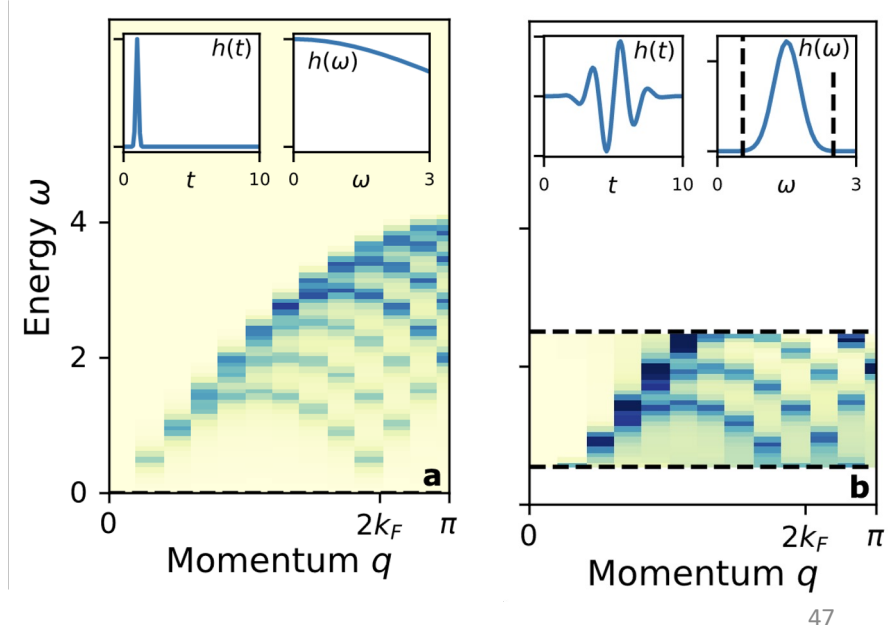


$$A(t) = A \int dt' \mathbb{X}^R \chi^R(t') h(t') + \mathcal{O}(h^{3/2})$$

$$\chi(r, t) = -i \langle \psi_0 | \delta n(r, t) \delta n(r=0, t=0) | \psi_0 \rangle$$

Measure density
on all sites

Wiggle potential
on site 0



Fermionic Linear Response

$$\frac{\delta A(t)}{\delta h(t')} \Big|_{h=0} = -i\theta(t-t') \langle \psi_0 | [\mathbf{A}(t), \mathbf{B}(t')] | \psi_0 \rangle$$

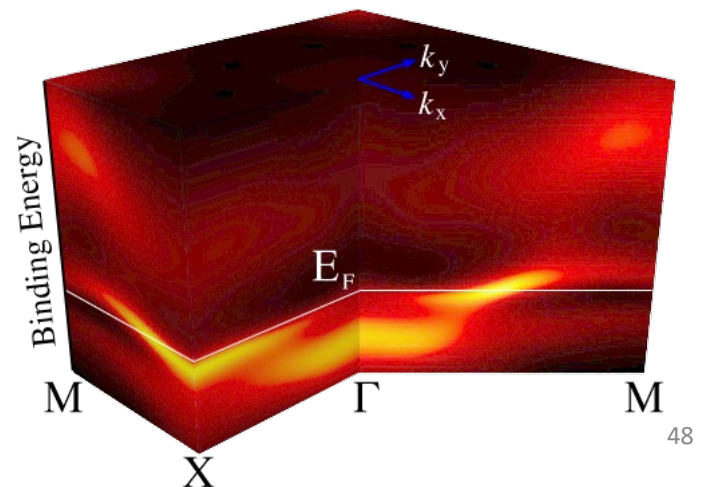
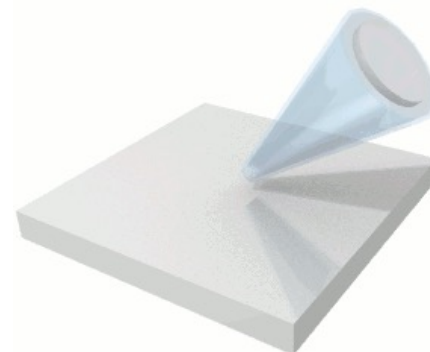
Notice this is a commutator...
... we might also want to have an anti-commuter

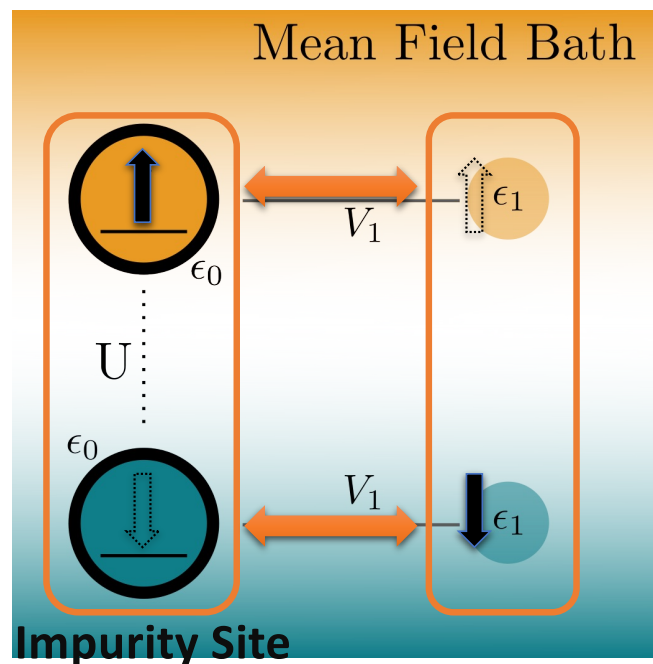
$$G(t, t') = -i\theta(t-t') \langle \psi_0 | \{ \mathbf{A}(t), \mathbf{B}(t') \} | \psi_0 \rangle$$

Why?

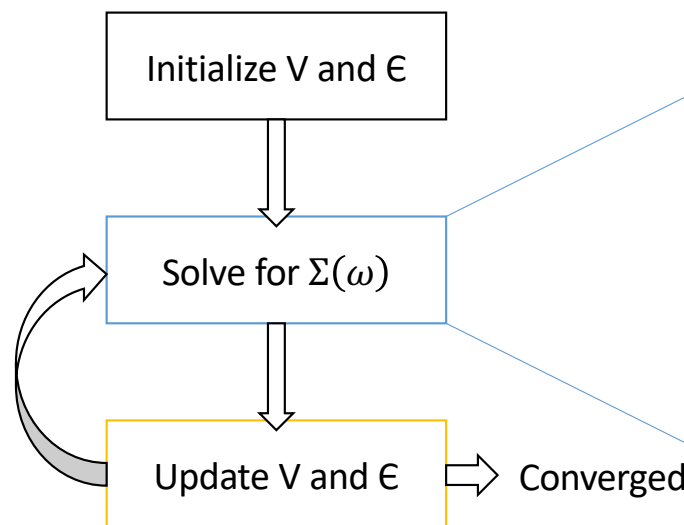
$$G^R(r_i, t; r_j, t') = -i\theta(t-t') \langle \psi_0 | \{ c_i(t), c_j^\dagger(t') \} | \psi_0 \rangle$$

Fermionic creation/
annihilation operators





Simplified DMFT Loop



On a Quantum Computer:

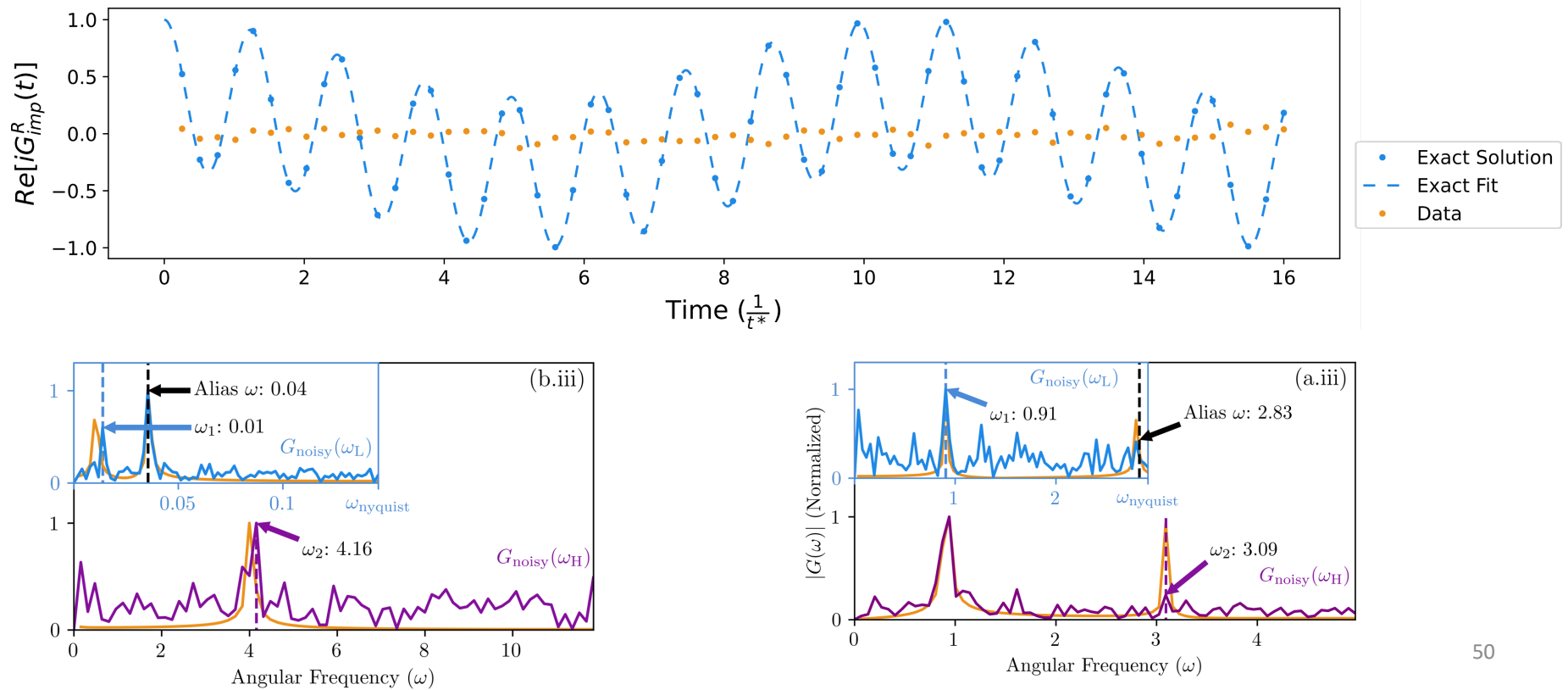
- 1) Compute Green's Function $G(t)$
- 2) Evaluate $G(\omega)$ and $\Sigma(\omega)$ via Fourier Transform
- 3) Solve for $Z = 1 - \frac{d}{d\omega} \Sigma(\omega)|_{\omega=0}$
- 4) $V = \sqrt{Z}$

Application of Green's functions: DMFT

[T. Steckmann et al., arXiv:2112.05688](#)

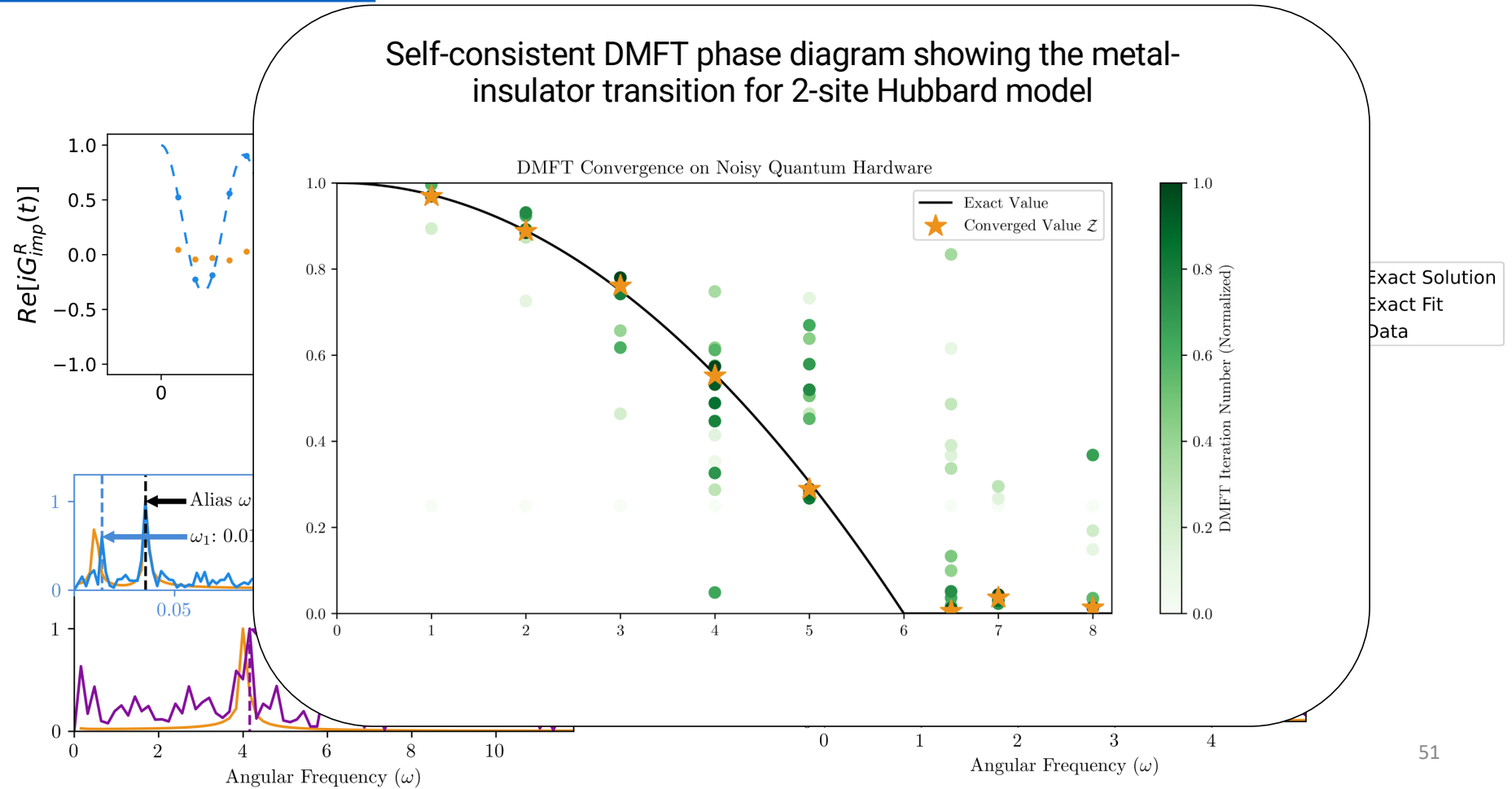
2-site Hubbard DMFT (5 qubits)

Cartan Based Simulation on IBM Lagos



2-site Hubbard DMFT

T. Steckmann et al., arXiv:2112.05688



Even More Mathematics... Are we done yet?

$$G(t, t') = -i\theta(t - t') \langle \psi_0 | \{ \mathbf{A}(t), \mathbf{B}(t') \} | \psi_0 \rangle$$

Even More Mathematics... Are we done yet?

$$G(t, t') = -i\theta(t - t') \langle \psi_0 | \{ \mathbf{A}(t), \mathbf{B}(t') \} | \psi_0 \rangle$$

- The method relies on the following identity:

$$[\mathbf{A}(t)\mathbf{P}, \mathbf{B}(t')] = \cancel{\mathbf{A}(t)\{\mathbf{P}, \mathbf{B}(t')\}} - \{\mathbf{A}(t), \mathbf{B}(t')\}\mathbf{P}$$

- If \mathbf{P} satisfies $\{\mathbf{B}(t), \mathbf{P}\} = 0$, $\mathbf{P}|\psi_0\rangle = s|\psi_0\rangle$ with $s \neq 0$

$$\begin{aligned} \langle \psi_0 | [\mathbf{A}(t)\mathbf{P}, \mathbf{B}(t')] | \psi_0 \rangle &= -\langle \psi_0 | \{ \mathbf{A}(t), \mathbf{B}(t') \} \mathbf{P} | \psi_0 \rangle \\ &= -s \langle \psi_0 | \{ \mathbf{A}(t), \mathbf{B}(t') \} | \psi_0 \rangle \end{aligned}$$

$$G(t, t') = \frac{i}{s} \theta(t - t') \langle \psi_0 | [\mathbf{A}(t)\mathbf{P}, \mathbf{B}(t')] | \psi_0 \rangle$$

Even More Mathematics... Are we done yet?

- Finally, if \mathbf{P} satisfies $[\mathcal{H}_0, \mathbf{P}] = 0$, we have $\mathbf{P} = \mathbf{P}(t)$, which leads to

$$G(t, t') = -i\theta(t - t')\langle\psi_0|\{\mathbf{A}(t), \mathbf{B}(t')\}|\psi_0\rangle$$

$$= \boxed{\frac{i}{s}\theta(t - t')\langle\psi_0|[\mathbf{A}(t)\mathbf{P}(t), \mathbf{B}(t')]|\psi_0\rangle}$$

- This allows us to measure anti-commutators via the previous method

Example: retarded Green's function

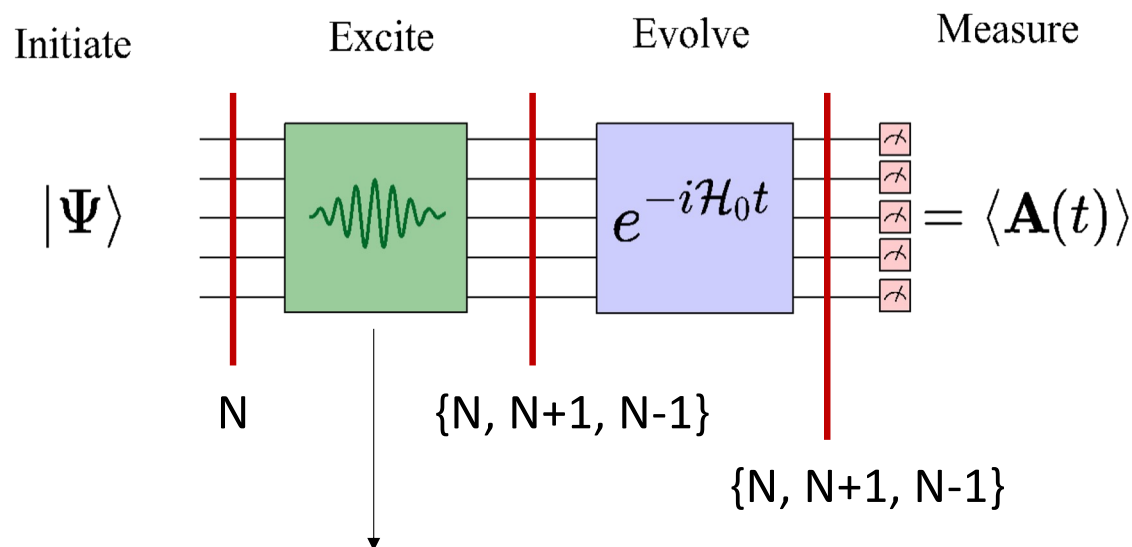
$$G^R(r_i, t; r_j, t') = -i\theta(t - t') \langle \psi_0 | \{c_i(t), c_j^\dagger(t')\} | \psi_0 \rangle$$

- The operator $\mathbf{P} = Z_1 Z_2 \dots Z_n$ satisfies $\{\mathbf{B}(t), \mathbf{P}\} = 0$
- For systems that preserves particle number parity: $[\mathcal{H}_0, \mathbf{P}] = 0$
- If state $|\psi_0\rangle$ has definite parity (even or odd particle number), then $\mathbf{P}|\psi_0\rangle = s|\psi_0\rangle$ with $s = +1$ or -1
- This works both for particle conserving and superconducting systems

Option 2: Post selection method:

Option 2: Post selection method:

- Assume that the Hamiltonian is particle conserving, and the ground state has a definite number of particles (which we denote with N).



$$\mathbf{B} = \eta (c + c^\dagger)$$

$$\mathbf{A} = \eta (c + c^\dagger)$$

Post-selection on particle number gives us

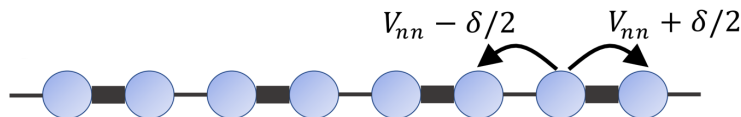
$$G_{ij}^<(t) = i \langle \psi_0 | c_j^\dagger(0) c_i(t) | \psi_0 \rangle$$

$$G_{ij}^>(t) = -i \langle \psi_0 | c_i(t) c_j^\dagger(0) | \psi_0 \rangle$$

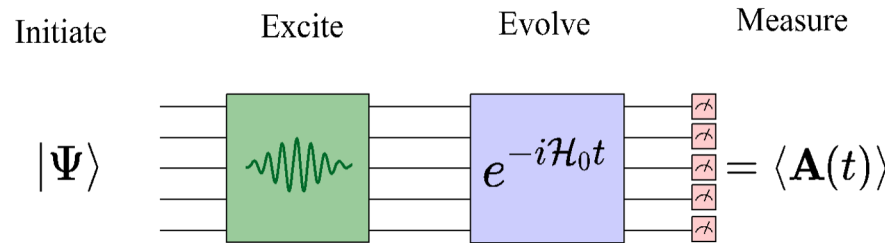
Which we can combine to the desired anti-correlation function.

Linear Response -> Green's function

Su-Schrieffer-Heeger model for polyacetylene



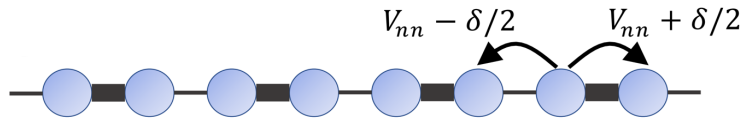
$$\mathcal{H}_0 = - \sum_{\langle i,j \rangle} \left[V_{nn} + (-1)^i \delta/2 \right] c_i^\dagger c_j - \mu \sum_i c_i^\dagger c_i$$



$$G^R(r_i, t; r_j, t') = -i\theta(t - t') \langle \psi_0 | \{c_i(t), c_j^\dagger(t')\} | \psi_0 \rangle$$

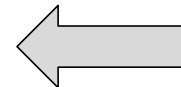
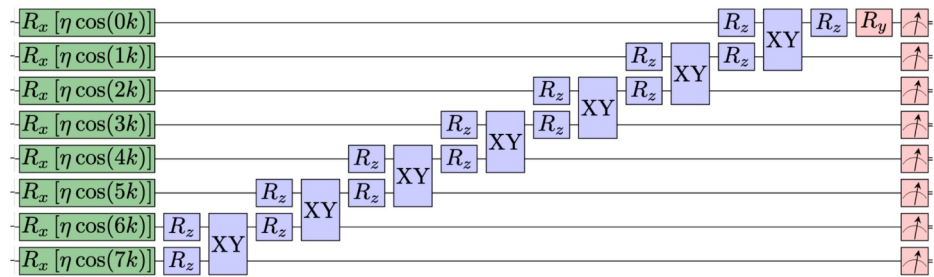
Linear Response -> Green's function

Su-Schrieffer-Heeger model for polyacetylene



$$\mathcal{H}_0 = - \sum_{\langle i,j \rangle} \left[V_{nn} + (-1)^i \delta/2 \right] c_i^\dagger c_j - \mu \sum_i c_i^\dagger c_i$$

Compressed circuit run on *ibm_auckland*



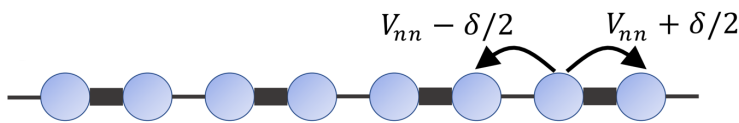
$$\mathbf{B} = \sum_i 2 \cos(kr_i) \left[c_i + c_i^\dagger \right]$$

Choose \mathbf{B} to create a momentum eigenstate

$$G_k^R(t) = -i\theta(t) \langle \psi_0 | \{c_k(t), c_k^\dagger(0)\} | \psi_0 \rangle$$

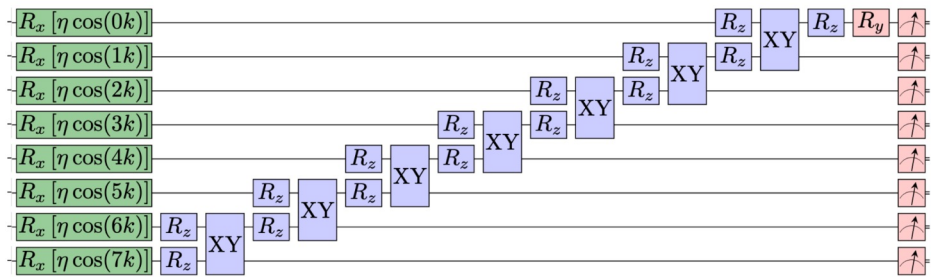
Linear Response -> Green's function

Su-Schrieffer-Heeger model for polyacetylene



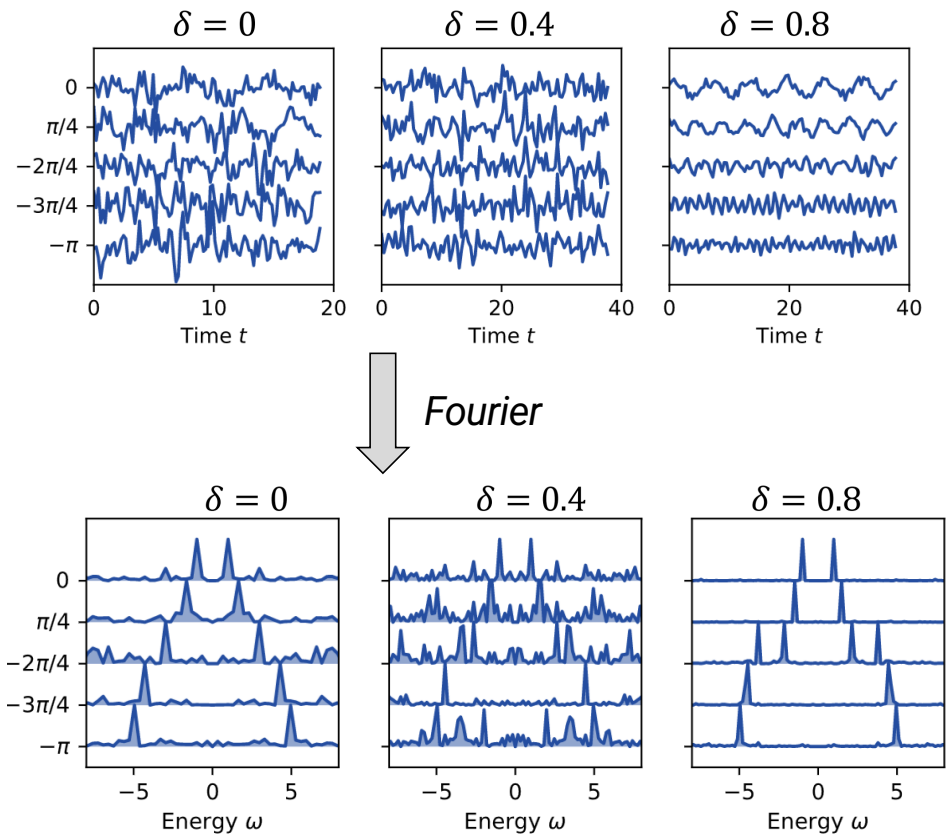
$$\mathcal{H}_0 = - \sum_{\langle i,j \rangle} \left[V_{nn} + (-1)^i \delta/2 \right] c_i^\dagger c_j - \mu \sum_i c_i^\dagger c_i$$

Compressed circuit run on *ibm_auckland*



Choose **B** to create a momentum eigenstate

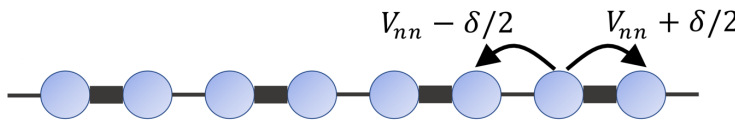
$$G_k^R(t) = -i\theta(t)\langle\psi_0|\{c_k(t), c_k^\dagger(0)\}|\psi_0\rangle$$



Linear Response -> Green's function

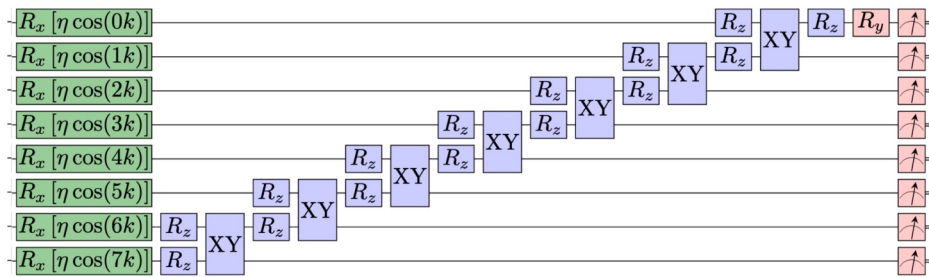
2302.10219

Su-Schrieffer-Heeger model for polyacetylene



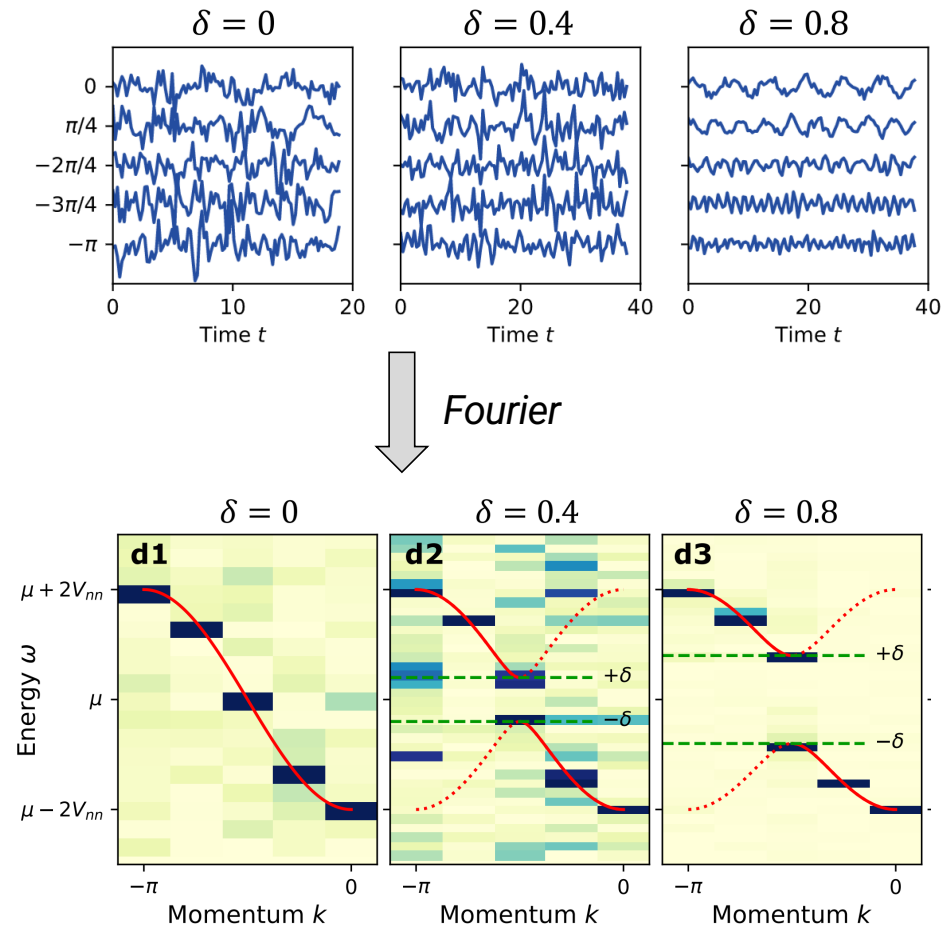
$$\mathcal{H}_0 = - \sum_{\langle i,j \rangle} \left[V_{nn} + (-1)^i \delta/2 \right] c_i^\dagger c_j - \mu \sum_i c_i^\dagger c_i$$

Compressed circuit run on *ibm_auckland*

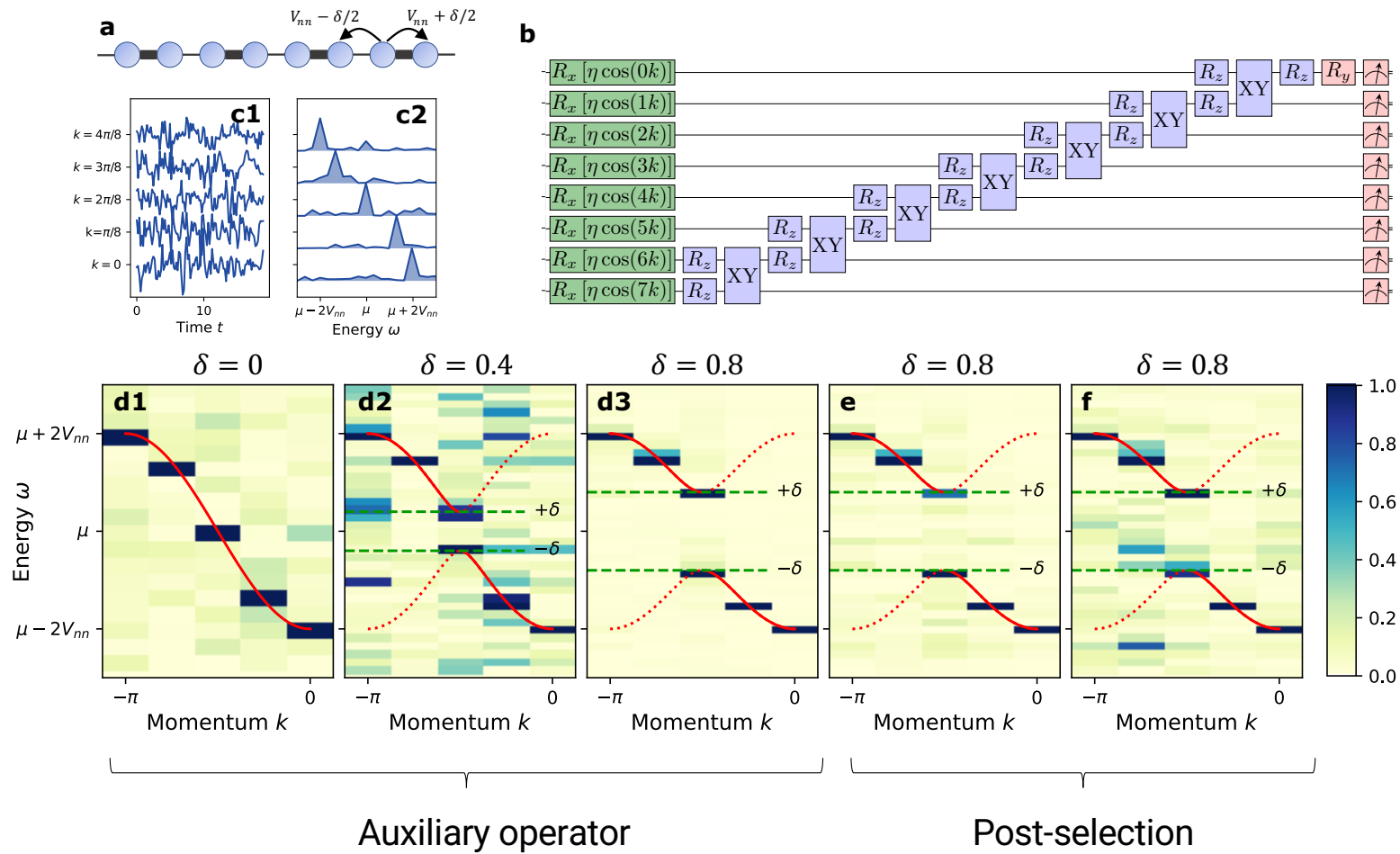


Choose **B** to create a momentum eigenstate

$$G_k^R(t) = -i\theta(t)\langle\psi_0|\{c_k(t), c_k^\dagger(0)\}|\psi_0\rangle$$



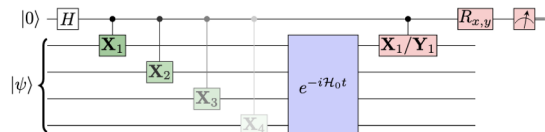
Linear Response -> Green's function



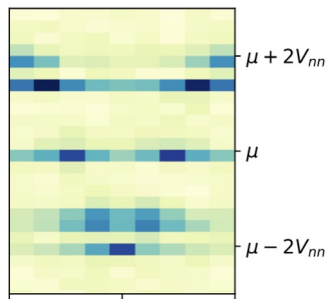
Linear Response -> Green's function

Why does this work so well?

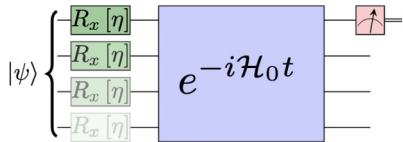
Hadamard test method



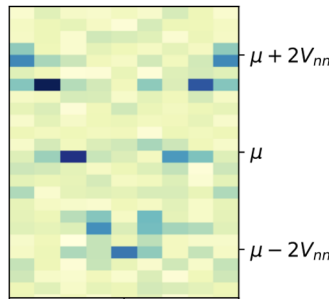
$\xrightarrow{\text{FT}}$
 $t \rightarrow \omega$
 $r \rightarrow k$



Position-selective linear response

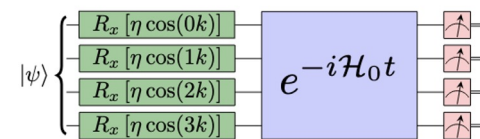


$\xrightarrow{\text{FT}}$
 $t \rightarrow \omega$
 $r \rightarrow k$

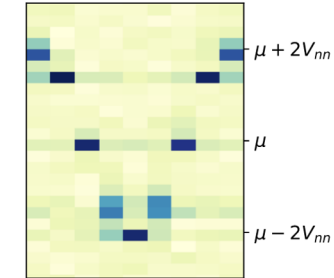


$$\mathbf{B} = \sum_i 2 \cos(kr_i) [c_i + c_i^\dagger]$$

Momentum-selective linear response

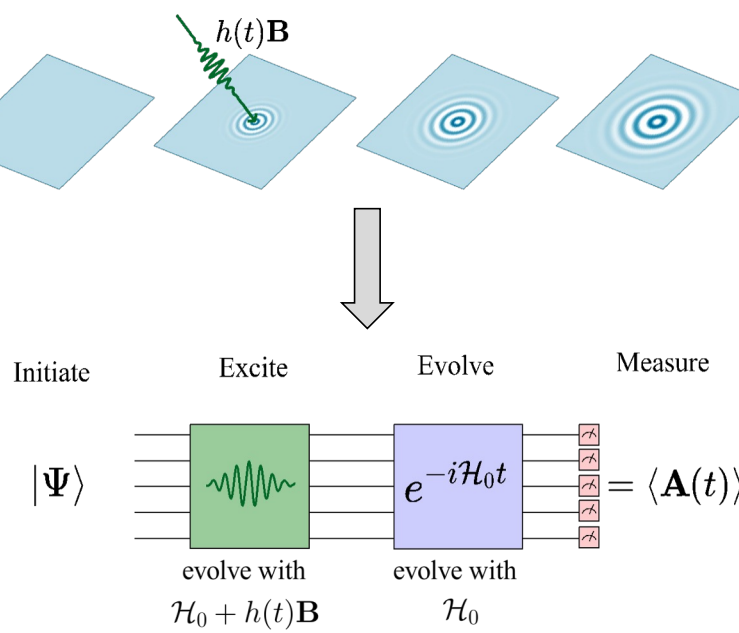


$\xrightarrow{\text{FT}}$
 ω

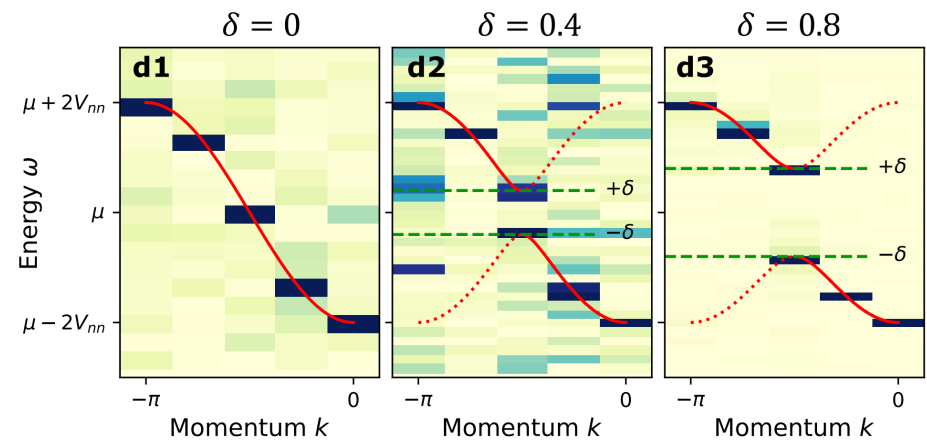


Data from noisy simulator with one/two qubit noise of 1% and 10%

Linear Response

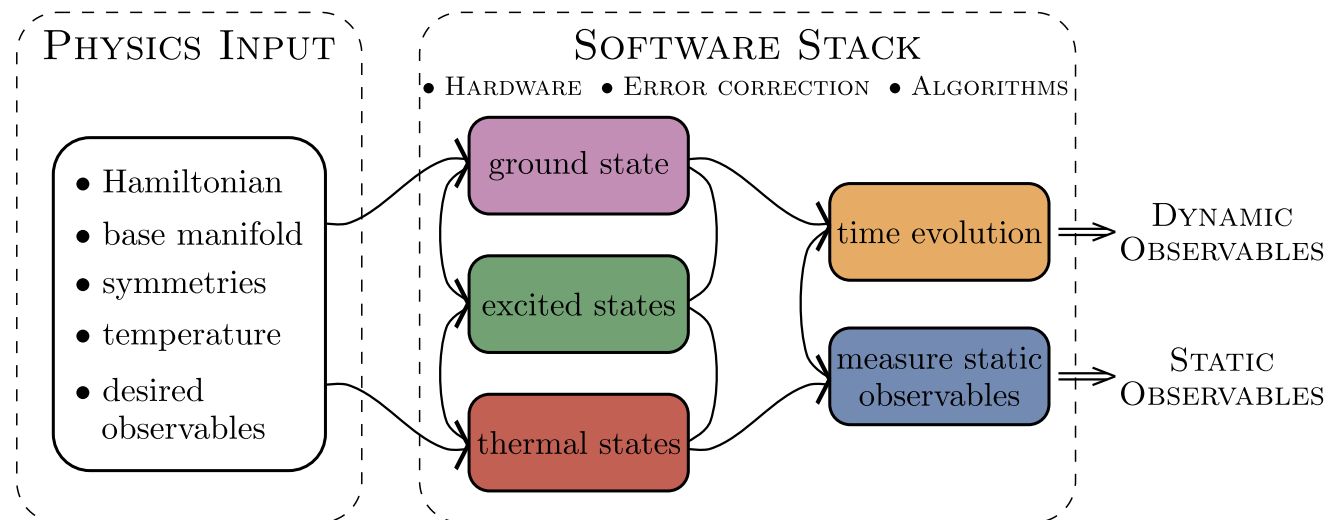


- Ancilla free
- Momentum and frequency selectivity
- Both bosonic and fermionic correlators
- More noise robust compared to existing methods

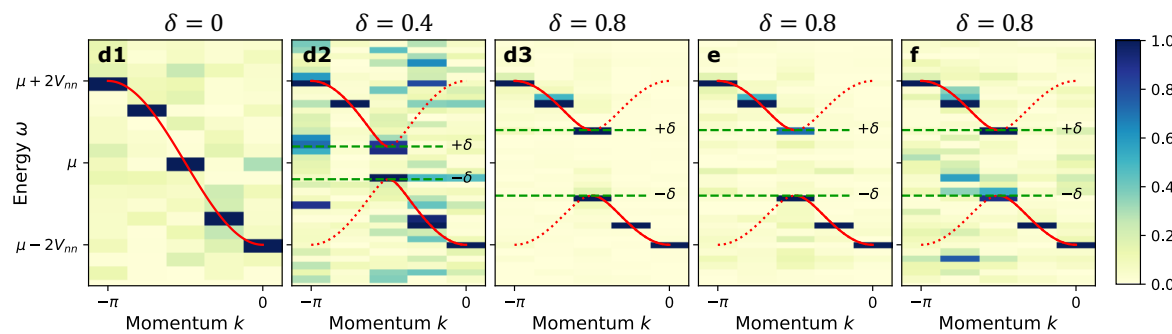


E. Kökcü, H. Labib, J.K. Freericks, AFK., arXiv:2302.10219

Quantum Matter meets Quantum Computing



<https://go.ncsu.edu/kemper-lab>



- Experimental relevance: Measuring correlation functions
- Measuring exact integer Chern numbers for topological states
- Driven/dissipative systems and fixed points (1000 Trotter steps)
- Time evolution via Lie algebraic decomposition and compression
- Thermodynamics via Lee-Yang Zeros
- Physics-Informed Subspace Expansions